

2020-01-01

Mathematical Modeling Of Microemulsification Processes, Numerical Simulations And Applications To Drug Delivery

Ogochukwu Nneka Ifeacho
University of Texas at El Paso

Follow this and additional works at: https://scholarworks.utep.edu/open_etd



Part of the [Mathematics Commons](#), and the [Physics Commons](#)

Recommended Citation

Ifeacho, Ogochukwu Nneka, "Mathematical Modeling Of Microemulsification Processes, Numerical Simulations And Applications To Drug Delivery" (2020). *Open Access Theses & Dissertations*. 3099.
https://scholarworks.utep.edu/open_etd/3099

This is brought to you for free and open access by ScholarWorks@UTEP. It has been accepted for inclusion in Open Access Theses & Dissertations by an authorized administrator of ScholarWorks@UTEP. For more information, please contact lweber@utep.edu.

MATHEMATICAL MODELING OF MICROEMULSIFICATION PROCESSES,
NUMERICAL SIMULATIONS AND APPLICATIONS TO
DRUG DELIVERY

OGOCHUKWU NNEKA IFEACHO

Master's Program in Mathematical Sciences

APPROVED:

Natasha S. Sharma, Ph.D., Chair

Joe Guthrie, Ph.D.

Jorge A. Munoz, Ph.D.

Stephen Crites, Ph.D.
Dean of the Graduate School

©Copyright

by

Ogochukwu N. Ifeacho

2020

To

my late mum, Peace Ogochukwu Ifeacho, 'Ojiugo nwanji'.

I will eternally be grateful to you for making me the woman I am today.

MATHEMATICAL MODELING OF MICROEMULSIFICATION PROCESSES,
NUMERICAL SIMULATIONS AND APPLICATIONS TO
DRUG DELIVERY

by

OGOCHUKWU NNEKA IFEACHO

THESIS

Presented to the Faculty of the Graduate School of

The University of Texas at El Paso

in Partial Fulfillment

of the Requirements

for the Degree of

MASTER OF SCIENCE

Department of Mathematical Sciences

THE UNIVERSITY OF TEXAS AT EL PASO

August 2020

Acknowledgements

Foremost, I would like to express my profound gratitude to my advisor Dr. Natasha S. Sharma. It definitely would not have been possible to complete this Thesis without her patience, motivation, guidance, vast knowledge and tutelage. I could not have imagined a better advisor and mentor to guide me through this my thesis-writing experience.

Besides my advisor, my immense gratitude goes out to the rest of my thesis committee: Prof. Joe Guthrie and Prof. Jorge A. Munoz for their encouragement, insightful comments and constructive criticisms.

I would like to acknowledge the support of the Texas Advanced Computing Center (TACC) at The University of Texas at Austin for providing HPC, visualization, database, or grid resources that have contributed to the research results reported within this thesis.

My sincere thanks goes to my family: to my dad, Engr. Francis C. Ifeacho who has always been my biggest fan and the major influence behind my studying Mathematics. To my late mum, Mrs Ogochukwu Ifeacho (Snr.) who sacrificed a lot for me to be where I am today and also whose boundless love radiates in us all. To my wonderful brothers; Engr. Francis C. Ifeacho (Jnr.), Engr. Ugochukwu Ifeacho and Chukwuma Ifeacho who are my support team and soldiers (ndi o ga-adiri mma).

I thank my amazing friend and colleague Mandela Bright Quashie for always being in my corner, helping and tutoring me in my weak areas. To Ada Benjamin Izundu, my friend turned sister, for her constant check-ups, words of wisdom and encouragement.

Of course, this acknowledgement will not be complete without mentioning my high school Mathematics teachers; Mrs. Chinyere Amalahu-Oguoma, Mr. Chinedu Obasi and Mr.

Obodo. They laid a good foundation right from the start which roused my affinity for Mathematics.

Finally, I want to thank God almighty without whom this Thesis would not have been successful in the first place.

Abstract

Microemulsion systems are a great pharmaceutical tool for the delivery of formulations containing multiple hydrophilic and hydrophobic ingredients of varying physicochemical properties. These systems are gaining popularity because of its long shelf life, improved drug solubilisation capacity, easy preparation and improvement of bioavailability. Despite the advantages associated with the use of microemulsion systems in pharmaceutical industries, the major challenge impeding their use has been and continues to be the lack of understanding of these systems.

Microemulsions can be mathematically modeled by an initial boundary value problem involving a sixth order nonlinear time dependent equation. In this thesis, we present a numerical method simulating the process of microemulsions. Relying on the mathematical model proposed by Gommper et. al [8], we show that our numerical method successfully captures the microemulsification process and is uniquely and unconditionally solvable. While we use the C^0 Interior Penalty finite element method for the spatial discretization, the time discretizations are based on a modified convex splitting of the energy of the systems.

Contents

	Page
Table of Contents	viii
Chapter	
1 Introduction	1
1.1 Phase Separation	2
1.2 Microemulsions	3
1.3 Conservation Law	6
1.4 Convex Splitting Scheme for Cahn-Hilliard Equation	8
1.5 Thesis Outline	8
2 Mathematical Preliminaries	11
2.1 Notation	11
2.2 Definitions, Lemmas and Theorems	12
2.3 Euler Lagrange Equations for membrane problem	15
2.4 The Finite Element Method	20
2.4.1 Importance of the Finite Element Method	22
3 A C^0 Interior Penalty Finite Element Method	26
3.0.1 History of the C^0 IP method	27
3.0.2 Derivation of the C^0 IP method	27
3.0.3 Continuity of $\mathbf{A}_h(\mathbf{u}_h, \mathbf{v}_h)$	33
3.0.4 Coercivity of $\mathbf{A}_h(\mathbf{u}_h, \mathbf{v}_h)$	35
3.0.5 Quality of the Solutions	36
4 Fully Discrete Convex Splitting Scheme	39
4.1 Weak Form	39
4.2 Time Discretization	40
4.2.1 Fully Discrete C^0 Interior Penalty Method	41

4.3 Unconditional Unique Solvability	43
5 Numerical Results	48
5.0.1 Accuracy Test	48
5.0.2 Formation of oil-in-water and water-in-oil droplets	49
6 Conclusion	53
6.1 Significance of the Result	53
6.1.1 Significance of Mathematical Modeling of Microemulsions	53
6.1.2 Applications of Microemulsions in Drug Delivery	53
6.2 Future Work	54
Appendices	57
A	58
B	59
C	61
Curriculum Vitae	64

Chapter 1

Introduction

Microemulsions form when a surfactant or more commonly a mixture of surfactants and/or co-surfactants, lowers the interfacial tension to ultra-low values, permitting the thermal motions to spontaneously disperse the two immiscible phases.

Depending on the phase, there are two types of microemulsions: water-in-oil (w/o) and oil-to-water (o/w). For microemulsions, the size of the droplets of the dispersed phase ranges between 5 and 100nm while that of macroemulsion is greater than 100 nm.

Microemulsions at the molecular scale are a finely even system. Here, the energetics of entropy and surface energies are opposing each other. The increment in entropy system depends of the higher number of droplets dispersed. This starts out as the most simple form where oil, water surfactant are mixed in different ratios and then the formed phases are tracked. Accordingly, single phases when spherical oil droplets are dispersed in water and the other where spherical water droplets are dispersed in oil. The change of these droplets may be from spherical to cylindrical or to worm-like micelle e.t.c [14]. Some instrumental techniques like nuclear magnetic resonance, dynamic light scattering, X-ray scattering e.t.c and their derivatives are widely used to study and carry out related experimentations on microemulsions.

These microemulsion systems are highly useful and have several key applications which span a lot of areas including drug delivery, food, fuel, consumer and industrial cleaning formulations, polymerization, cosmetics, agrochemicals e.t.c.

Microemulsions are thermodynamically stable, fluid and optically clear dispersions of two immiscible liquids such as oil and water. This is basically done by the dispersion of droplets of one liquid into the other. These droplets are called the *dispersed phase* while the

second liquid is the *continuous phase*.

To describe the microemulsification process, we first introduce the model of phase separa-

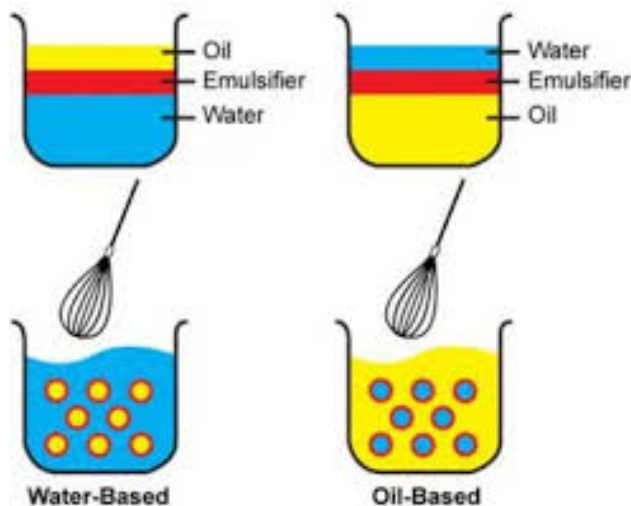


Figure 1.1: Whisking an emulsion of oil-in-water (left) and water-in-oil (right).

tion described by the fourth order Cahn-Hilliard equation and then, derive the sixth-order Cahn-Hilliard equation modeling the microemulsification process.

1.1 Phase Separation

Consider two immiscible liquids oil and water confined to a region $\Omega \subset \mathbb{R}^2$, as described in Figure 1. In the absence of any mixing, there are two distinct phases oil-rich phase $\phi_o = -1$ and water-rich phase $\phi_w = 1$. This can be mathematically described by means of

$$\phi : \Omega \rightarrow \mathbb{R}, \quad \phi = -1 \text{ in } \Omega_o \subset \Omega \quad \text{indicates an oil-rich region.}$$

Similarly, $\phi = 1$ in $\Omega_w \subset \Omega$ indicates the water-rich region. It is known that at high temperatures, we achieve a uniform mixing/distribution of the volume fractions (50-50 mixture of water and oil indicated by $\phi = 0$). Upon cooling this solution, below a certain temperature, the solution separates into oil-rich and water-rich phase one observes that while the total volume of oil and water stays the same, some regions occupied by oil shrink

and those occupied by water grow and vice versa. This describes the phenomena of spinodal decomposition investigated by Cahn and Hilliard [?] and with associated energy of the fluid given by

$$E(\phi) = \int_{\Omega} \left[\frac{1}{\epsilon} f(\phi) + \frac{\epsilon}{2} |\nabla\phi|^2 \right] dx, \tag{1.1}$$

where

- $f(\phi) = \frac{1}{4}(\phi^2 - 1)^2$ denotes the bulk energy associated with the propensity of separation into the pure states ± 1 ,
- $\frac{\epsilon}{2} |\nabla\phi|^2$ denotes the gradient energy density associated with the interfacial energy depicting the tendency to mix.

Note that if $\phi = \pm 1$ then, $\nabla\phi = 0$ so in the regions of pure states, this term vanishes.

The pure phases are separated by a diffuse interface of thickness ϵ . In order to model the interface between two phases, phase field models, such as the use of the Cahn-Hilliard equation, place a diffuse interface between the phases of the system. This also allows for a natural description of topological changes in the model, without relying on any additional input from the user.

1.2 Microemulsions

To induce an emulsification, a surfactant/emulsifier is added to this system. A surfactant is a surface active molecule which exhibits an amphiphilic nature; with a coexistence of a hydrophilic (water-loving) and a lipophilic (fat-loving) component. When a small amount of amphiphilic molecules is added to a phase separated mixture of oil and water, a homogeneous microemulsion phase forms at $\phi = 0$. (See Figure below.)

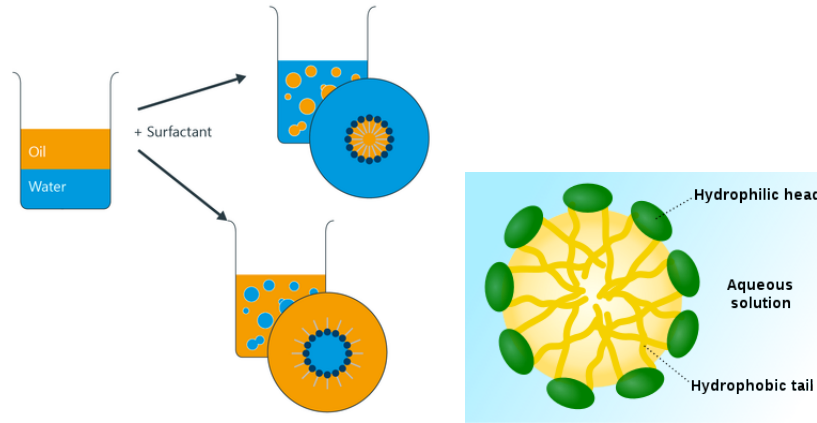


Figure 1.2: Left: Adding surfactant to a composition of water-oil. Right: This surfactant contains both hydrophobic or lipophilic (fat-loving tail) and hydrophilic (water-loving head) properties

Derivation of Mathematical Model

According to Gompper and Zschocke 91 [9], there are two approaches to understand the oil-water-surfactant mixture systems and their properties. These can be described as:

1. Microscopic approach: molecules and their interaction. Here the variables in this theory are the local concentrations of the molecules.
2. Interfacial approach: the amphiphiles form monolayers at the microscopic oil-water interface. Since the monolayers are almost incompressible their area is almost constant so that their interfacial fluctuations are controlled by the elastic bending energy.

Relying on the Ginzburg-Landau free energy functional, there are two order parameters: ϕ and τ that describe the free energy functional. Here ϕ is a scalar order parameter which is proportional to the local difference of the oil and water concentration. While τ characterizes surfactant and τ points in the direction of the heads of surfactant molecules. Assuming that the interface thickness is of the same order as the length of a surfactant molecules and that the surfactant molecules are aligned exactly along the local interface normal \mathbf{n} that is

$\tau = \tau_0 \mathbf{n}$ where τ_0 is the surfactant density at the interface, the free energy functional is of the form:

$$E(\phi) = F_0(\phi) + G_0(\phi) \quad (1.2)$$

where $\kappa_2 > 0$,

$$G_0(\phi) = \underbrace{\int_{\Omega} \left\{ \frac{\kappa_1(\phi)}{2} |\nabla \phi|^2 + \frac{\kappa_2}{2} (\Delta \phi)^2 \right\} dx}_{\text{tendency to mix}},$$

and

$$F_0(\phi) = \underbrace{\frac{\beta}{2} \int_{\Omega} (\phi - \phi_o)^2 (\phi^2 + h_0) (\phi - \phi_w)^2 dx}_{\text{interaction to separate}} \quad (1.3)$$

with $\beta > 0$ is surface energy density and the parameter h_0 measures the deviation from the oil-water-microemulsion coexistence. $F_0(\cdot)$ has three local extrema at the oil-rich phase $\phi = \phi_o = -1$, the water-rich phase $\phi = \phi_w = 1$ and the microemulsion phase $\phi = 0$ respectively.

Remark 1.2.1. We note that the properties of the surfactant and its concentration are expressed through $F_0(\phi)$ and $\kappa_1(\phi)$. The latter term is determined experimentally to be a second order polynomial $\kappa_1(\phi) = a_0 + a_2 \phi^2$. For more details of the (neutron-scattering) experiments used to determine $\kappa_1(\phi)$ see [16] and [17]. Thus,

$$G_0(\phi) = \int_{\Omega} \left\{ \frac{a_0 + a_2 \phi^2}{2} |\nabla \phi|^2 + \frac{\kappa_2}{2} (\Delta \phi)^2 \right\} dx.$$

Remark 1.2.2. The energy functional (1.2) is similar to phase separation energy (1.1) except for having an additional term which measures the bending energy $\frac{\kappa_2}{2} (\Delta \phi)^2$ of the energy $E(\phi)$ in (1.2) and, $F_0(\phi)$ which introduces a microemulsion state through the additional term $(\phi^2 + h_0)$. In the absence of amphiphilic molecules $F_0(\phi)$ possesses only two states namely oil-rich and water-rich at ϕ_o and ϕ_w respectively.

Remark 1.2.3. If $\kappa_1(\phi) = a_0$ and $\kappa_2 = 0$, and $F_0(\cdot)$ is adjusted accordingly, then the energy functional $E(\phi)$ represents classical Cahn-Hilliard free energy (1.1).

$$E(\phi) = \frac{a_0^{-1}}{4} \int_{\Omega} (\phi + 1)^2 (\phi - 1)^2 dx + \int_{\Omega} \frac{a_0}{2} |\nabla \phi|^2 dx. \quad (1.4)$$

1.3 Conservation Law

Since the order parameter ϕ is a conserved quantity, it satisfies the following conservation law:

$$\partial_t \phi + \nabla \cdot \mathbf{j} = 0 \quad (1.5)$$

with mass flux \mathbf{j} given by

$$\mathbf{j} = -M \nabla \mu,$$

where $M \equiv M(\phi) = 1 > 0$ is a mobility, μ is the chemical potential differences between the phases defined as the first variation of the free energy $\delta_{\phi} E$.

Conservation Law for phase separations

Set $\Omega \subset \mathbb{R}^2$ is a bounded domain occupied by the binary mixture. For phase separation phenomena, the energy functional E is given by (1.1). The conservation law assumes the form of the fourth order Cahn-Hilliard equation (1.6)-(1.8) and which capturing the dynamics of phase separation.

$$\partial_t \phi - \nabla \cdot (M \nabla \mu) = 0, \quad \text{in } \Omega \times (0, T) \quad (1.6)$$

$$\mu := \delta_{\phi} E = \epsilon^{-1} (\phi^3 - \phi) - \epsilon \Delta \phi = 0 \quad \text{in } \Omega \times (0, T), \quad (1.7)$$

$$\partial_n \phi = \partial \mu = 0 \quad \text{on } \partial \Omega \times (0, T), \quad (1.8)$$

where T denotes final time, M denotes the mobility function, μ denotes the chemical potential and $\delta_{\phi} E$ denotes the variational derivative of E with respect to ϕ . The details of the calculation of $\delta_{\phi} E$ is provided in Appendix B.

We note that the minimizing function ϕ satisfies the which represent the Cahn-Hilliard equation

Conservation Law for microemulsions

Now, let $\Omega \subset \mathbb{R}^2$ is a bounded domain occupied by the ternary mixture. For microemulsions, the energy functional E is given by (1.2). Furthermore, the chemical potential is

$$\mu := \delta_\phi E = f_0(\phi) - \kappa_1(\phi)\Delta\phi - a_2\phi|\nabla\phi|^2 + \kappa_2\Delta^2\phi, \quad (1.9)$$

where $\kappa_1(\phi) = a_0 + a_2\phi^2$, $a_2 > 0$ and $f_0(\phi) := \delta_\phi F_0(\phi)$. The details of the calculation of $\delta_\phi E$ is provided in Appendix C. We note that $f_0(\cdot)$ assumes the following form:

$$f_0(\phi) = \frac{\beta}{2} \left(6\phi^5 + 4(h_0 - 2)\phi^3 + 2(1 - 2h_0)\phi \right). \quad (1.10)$$

Thus, the system we end up with is:

$$\partial_t\phi - \nabla \cdot M\nabla\mu = 0, \quad (1.11)$$

$$f_0(\phi) - \kappa_1(\phi)\Delta\phi - a_2\phi|\nabla\phi|^2 + \kappa_2\Delta^2\phi - \mu = 0. \quad (1.12)$$

This system represents a system of DAE (Differential Algebraic equations) consisting of a linear second order evolutionary equation (1.11) and a fourth order nonlinear Cahn-Hilliard type equation (1.12). We set the parameters appearing in the system as:

- $h_0 = 0.5$, $\beta = 1/3$, $\kappa_2 = 1$;
- $\kappa_1(\phi) = a_2\phi^2 + a_0 = \phi^2 - 4$.

In view of of the above values, the system simplifies to:

$$\partial_t\phi - \nabla \cdot (\nabla\mu) = 0, \quad (1.13a)$$

$$\phi^5 - \phi^3 + \phi|\nabla\phi|^2 - \nabla \cdot (\phi^2\nabla\phi) + 4\Delta\phi + \Delta^2\phi - \mu = 0. \quad (1.13b)$$

1.4 Convex Splitting Scheme for Cahn-Hilliard Equation

The numerical scheme uses a modified energy splitting technique which was introduced by Eyre [7]. This scheme is first order accurate in time and results in an unconditionally energy stable and unconditionally uniquely solvable. The idea of this scheme is to decompose the energy $E(\phi)$ described by either (1.1) or (1.2) for the phase separation or microemulsions energy respectively into the difference of two convex energies:

$$E(\phi) = E_c(\phi) - E_e(\phi)$$

and to treat E_c implicitly while E_e explicitly. This has been successfully applied to developing a time stepping scheme for the fourth order Cahn-Hilliard equation where the splitting assumes the form

$$E_c(\phi) = \int_{\Omega} \left\{ \frac{\phi^4 + 1}{4\epsilon} + \frac{\epsilon |\nabla \phi|^2}{2} \right\} dx, \quad E_e(\phi) = \int_{\Omega} \frac{\phi^2}{2\epsilon} dx.$$

The above convex splitting does not however, apply to the energy associated with the microemulsions. As a consequence, we propose a new scheme derived from the Eyre's convex splitting scheme and will be discussed in Chapter 4.

1.5 Thesis Outline

The remaining thesis is organized as follows. In Chapter 2, we introduce useful notations, definitions and results including the finite element method for second order problem. In Chapter 3, we describe the C^0 Interior Penalty (IP) finite element method for the fourth order elliptic problem and then in Chapter 4, introduce the fully discrete modified convex time splitting finite element scheme. Our proposed numerical scheme is based on a variant of the Eyre's convex splitting scheme in conjunction with the C^0 interior penalty method [3]

and backward Euler for the space-time discretization. The main heart of the thesis lies in proving the unique solvability of the scheme presented in Chapter 4. Chapter 5 presents the numerical validation of our method and finally, we conclude the thesis in Chapter 6 with some future work directions. The table below lists the operators and function spaces used in this chapter.

Additional definitions of the differential operators such as ∇ , Δ^2 used throughout this thesis are provided in Appendix A.

Table 1.1: Operators and Function Spaces

Notations			
Chapters	S/No	Operators	Function Spaces
	1	$\Omega \subset R^d; d = 1, 2$: bounded domain/microemulsion region.	$L^2(\Omega)$: Hilbert Space of square integrable functions on Ω endowed with the norm: $\ f\ _p = (\int_{\Omega} f ^p)^{\frac{1}{p}}$.
	2	ϕ_0 : Oil-rich phase	$H^m(\Omega)$: Sobolev space of order 'm' on $\Omega = \{v \in L^2(\Omega); \partial_{x_i} \in L^2(\Omega) ; 1 \leq i \leq d\}$
	3	ϕ_w : Water-rich phase	$(\nabla^2 u : \nabla^2 v)$: inner product of the trace of Hessian Matrice of u and the trace of Hessian Matrix of v.
Chapter 1	4	ϕ : Scalar order parameter proportional to the local difference of oil and water concentration.	
	5	μ : chemical potential of the Free Energy Functional.	
	6	$\nabla u = \left(\frac{\partial}{\partial x} + \frac{\partial}{\partial y} \right) u$	
	7	$\nabla^2 u = \text{trace}(H(u))$ where $H(u)$ is the Hessian Matrix of u.	$H(u) = \begin{pmatrix} \frac{\partial^2 u}{\partial x_1^2} & \cdot & \cdot & \cdot & \frac{\partial^2 u}{\partial x_1 \partial x_n} \\ \frac{\partial^2 u}{\partial x_2 \partial x_1} & \cdot & \cdot & \cdot & \frac{\partial^2 u}{\partial x_2 \partial x_n} \\ \frac{\partial^2 u}{\partial x_n \partial x_1} & \cdot & \cdot & \cdot & \frac{\partial^2 u}{\partial x_n^2} \end{pmatrix}$ $\text{trace}(H(u)) = \frac{\partial^2 u}{\partial x_1^2} + \frac{\partial^2 u}{\partial x_2^2} + \dots + \frac{\partial^2 u}{\partial x_n^2} = \nabla^2 u$
	8	$\delta_{\phi} E = \lim_{\alpha \rightarrow 0} \frac{E(\phi + \alpha \Phi) - E(\phi)}{\alpha}$: The Gateaux Derivative of E w.r.t ϕ .	
	9	Δu : Laplacian operator	$(\nabla \cdot \nabla)u = \text{trace}(H(u))$.

Chapter 2

Mathematical Preliminaries

2.1 Notation

Table 2.1: Operators and Function Spaces

Notations			
Chapters	S/No	Operators	Function Spaces
	10	$\Gamma = \partial\Omega$: Piecewise smooth boundary of Ω .	$C(\Omega)$: the set of continuous functions on Ω .
	11	$D^\alpha = \frac{\partial^{\alpha_1}}{\partial x_1^{\alpha_1}}, \frac{\partial^{\alpha_2}}{\partial x_2^{\alpha_2}}, \dots, \frac{\partial^{\alpha_n}}{\partial x_n^{\alpha_n}}$	$C^k(\Omega)$: the set of continuous functions whose first k th derivatives are also continuous on Ω .
Chapter 2	12		$C_0(\Omega)$: The space of bounded real-valued continuous functions on Ω with compact support in Ω .
	13		$C_0(\bar{\Omega})$: The space of bounded real-valued continuous functions in $C_0(\Omega)$ on the closure of Ω with compact support in Ω .
	14		$H_0^k(\Omega)$: Sobolev spaces of order k with compact support in Ω .

2.2 Definitions, Lemmas and Theorems

Proper Convex Functionals

A functional $J : V \rightarrow \bar{R}$ is called convex if for all $u, v \in V$ and $\lambda \in [0, 1]$ there holds;

$$J(\lambda u + (1 - \lambda)v) \leq \lambda J(u) + (1 - \lambda)J(v)$$

J is proper convex if $J(v) > -\infty$, $v \in V$, and $J \neq +\infty$.

and strictly convex if;

$$J(\lambda u + (1 - \lambda)v) < \lambda J(u) + (1 - \lambda)J(v)$$

for all $u, v \in V$, $u \neq v$, and $\lambda \in [0, 1]$. See [11] for more details.

Coercive Functionals

A functional $J : V \rightarrow \bar{R}$ is said to be coercive if

$J(v) \rightarrow +\infty$ for $\|v\|_V \rightarrow +\infty$.

Gateaux Derivative

A functional $J : V \rightarrow \bar{R}$ is called Gateaux-differentiable in $u \in V$ if;

$$J'(u, v) = \lim_{\lambda \rightarrow 0^+} \frac{J(u + \lambda v) - J(u)}{\lambda}$$

exists for all $v \in V$. Moreover, if there exists $J' \in V^*$ such that

$$J'(u, v) = J'(u)(v) = \langle J'(u), v \rangle_{V^*, V}$$

$v \in V$, then $J'(u)$ is called the Gateaux-derivative of J in $u \in V$.

Sobolev Spaces

Let $\Omega \subseteq \mathbb{R}^2$ be a bounded domain and let $\alpha = (\alpha_1, \dots, \alpha_n)$ be a multi index of order $|\alpha| = \alpha_1 + \dots + \alpha_n = k$, define;

$$D^\alpha = \frac{\partial^{\alpha_1}}{\partial x_1^{\alpha_1}} \cdots \frac{\partial^{\alpha_n}}{\partial x_n^{\alpha_n}}$$

where the derivative is understood in the sense of weak derivatives. Sobolev semi-norms when k is a positive integer are defined as follows:

$$D^{(1,0)}u = \frac{\partial u}{\partial x}, \quad D^{(0,1)}u = \frac{\partial u}{\partial y} \quad \alpha = (0, 1) \text{ and } \alpha = (1, 0), \text{ with } |\alpha| = 1$$

Thus for $k = 1$,

$$|v|_{H^1(\Omega)}^2 = \sum_{|\alpha|=1} \|D^\alpha v\|_{L^2(\Omega)}^2$$

let v be C^∞ function on $\Omega \subseteq \mathbb{R}^2$. Then,

$$\begin{aligned} |v|_{H^1(\Omega)}^2 &= \|D^{(1,0)}v\|_{L^2(\Omega)}^2 + \|D^{(0,1)}v\|_{L^2(\Omega)}^2 \\ &= \int_{\Omega} \left| \frac{\partial v}{\partial x} \right|^2 dx dy + \int_{\Omega} \left| \frac{\partial v}{\partial y} \right|^2 dx dy \end{aligned}$$

For $k = 2$ we have;

$$\begin{aligned} |v|_{H^2(\Omega)}^2 &= \|D^{(2,0)}v\|_{L^2(\Omega)}^2 + \|D^{(0,2)}v\|_{L^2(\Omega)}^2 + \|D^{(1,1)}v\|_{L^2(\Omega)}^2 \\ &= \int_{\Omega} |\partial_x^2 v|^2 dx dy + \int_{\Omega} |\partial_y^2 v|^2 dx dy + \int_{\Omega} |\partial_x \partial_y v|^2 dx dy \end{aligned}$$

Semi Norm

$$|v|_{H^1(\Omega)} = 0 \implies \nabla v = 0 \text{ but } \nRightarrow v = 0$$

Poincaré Inequality holds true on Ω , i.e

$$\|v\|_{L^2(\Omega)} \leq c \|\nabla v\|_{L^2(\Omega)}$$

thus;

$$\begin{aligned} \|v\|_{H^1(\Omega)}^2 &= \|v\|_{L^2(\Omega)}^2 + \|D^{(1,0)}v\|_{L^2(\Omega)}^2 + \|D^{(0,1)}v\|_{L^2(\Omega)}^2 \\ &= \|v\|_{L^2(\Omega)}^2 + \|\partial_x v\|_{L^2(\Omega)}^2 + \|\partial_y v\|_{L^2(\Omega)}^2 \end{aligned}$$

note; $\|v\|_{H^1(\Omega)} = 0 \implies v = 0$ because $|\alpha| \leq 1$

Define the Sobolev Spaces $H^k(\Omega)$ as follows;

$$H^k(\Omega) = \{v \in L^2(\Omega) : \|v\|_{H^k(\Omega)} < +\infty\}$$

Define;

$$H_0^k(\Omega) = \{v \in H^k(\Omega) : D^\alpha v = 0 \text{ on } \partial\Omega \text{ for } |\alpha| < k\}$$

The following theorem states that $|\cdot|_{H^k(\Omega)}$ is a norm on $H_0^k(\Omega)$.

Theorem: Poincarè Inequality

Let Ω be a bounded polygonal domain. Then there exists a constant C such that;

$$\|v\|_{H^k(\Omega)} \leq C|v|_{H^k(\Omega)} \quad \forall v \in H_0^K(\Omega)$$

thus;

$$H_0^K(\Omega) \subset H^k(\Omega) \text{ such that } D^\alpha v = 0 \text{ for } |\alpha| < k$$

for $k = 2$;

$$\begin{aligned} H_0^2(\Omega) &= \{v \in H^2(\Omega) : D^\alpha v = 0 \text{ for } |\alpha| < 2, |\alpha| = 0 \text{ and } |\alpha| = 1\} \\ &= \{v \in H^2(\Omega) : v = 0 \text{ and } \frac{\partial v}{\partial x} = \frac{\partial v}{\partial y} = 0 \text{ on } \partial\Omega\} \end{aligned}$$

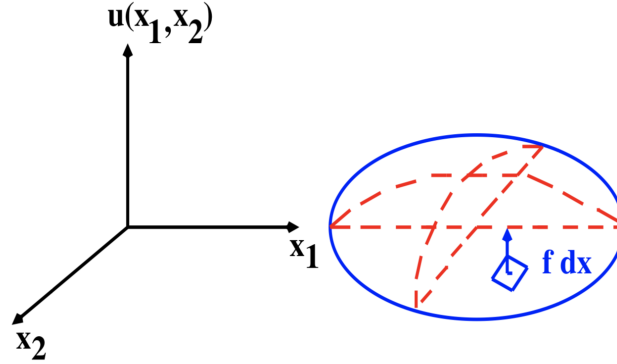


Figure 2.1: Deflection of a clamped membrane

2.3 Euler Lagrange Equations for membrane problem

In this section, we introduce the necessary and sufficient conditions for the existence of a minimizer to the energy functional associated with the microemulsions. It turns out that these conditions are the Euler Lagrange (EL) equations. Deriving these equations is important because they represent the optimality conditions for existence of the minimizer ϕ that minimizes the energy $E(\phi)$ functional. Furthermore, these EL equations are the building blocks for the finite element method we rely on to compute the energy minimizer.

We start this chapter by deriving the EL equations for a stationary membrane problem and then, present the finite element method for solving it. Finally, we present the EL equations for the existence of a minimizer to the energy functional associated with the microemulsions.

A membrane is a surface elastic body in its ground state whose potential energy is directly proportional to the change of the surface area. Here, the ground state is a bounded domain $\Omega \subset R^2$ with boundary $\Gamma = \partial\Omega$ which is assumed to be piecewise smooth.

Under the influence of an external force with density $f = f(x)$, $x \in \Omega$ which acts perpendicular to the (x_1, x_2) -plane, the membrane is deflected in the x_3 plane. There is no deflection for $x \in \Gamma$ since the membrane is clamped.

The equilibrium state is characterized as the physical state where the total energy of the membrane attains its minimum. Thus, the total energy for this system is

$$J = J_p - J_f \quad (2.1)$$

where J_p is the potential energy and J_f is the energy associated with the exterior force as seen in [11]. Since the potential energy is proportional to the change in surface area;

$$\int_{\Omega} (1 + |\nabla u|^2)^{\frac{1}{2}} dx - \int_{\Omega} dx \quad (2.2)$$

with the restriction $|\nabla u| \leq 1$, we obtain;

$$\int_{\Omega} (1 + |\nabla u|^2)^{\frac{1}{2}} dx - \int_{\Omega} dx = \int_{\Omega} dx + \frac{1}{2} \int_{\Omega} |\nabla u|^2 dx + o(|\nabla u|^2)$$

the $o(|\nabla u|^2)$ term is neglected resulting in;

$$J_p(u) = \frac{\mu}{2} \int_{\Omega} |\nabla u|^2 dx \quad (2.3)$$

where $\mu > 0$ is a material constant that reflects the elastic response of the membrane. Again,

$$J_f(u) = \int_{\Omega} fu \, dx \quad (2.4)$$

Thus the total energy from equations 2.3 and 2.4 yields:

$$J(u) = \frac{1}{2} \int_{\Omega} |\nabla u|^2 dx - \int_{\Omega} fu \, dx. \quad (2.5)$$

Minimization Problem

Our goal is to determine the displacement u that yields the minimum energy $J(u)$.

That is we seek $u \in H_0^1 \equiv H_0^1(\Omega)$ such that ;

$$J(u) = \inf_{v \in H_0^1} J(v) \quad (2.6)$$

Application to the Membrane Problem

We are required to show that the membrane problem (1.5) has a unique solution $u \in H_0^1(\Omega)$ that is the solution of the variational equation;

$$\mu \int_{\Omega} \nabla u \cdot \nabla v dx = \int_{\Omega} f v dx \quad \forall v \in H_0^1(\Omega). \quad (2.7)$$

Proof. Required to show that:

1. J is convex
2. $\langle J'(u), v \rangle = \mu \int_{\Omega} \nabla u \cdot \nabla v dx - \int_{\Omega} f v dx = 0$, $v \in V$.
3. There exists a unique solution $u \in H_0^1(\Omega)$ that is the solution to 2.7.

We first compute $\frac{J(u+\lambda v) - J(v)}{\lambda}$ as follows:

$$\begin{aligned} J(u + \lambda v) &= \frac{\mu}{2} \int_{\Omega} |\nabla(u + \lambda v)|^2 dx - \int_{\Omega} f(u + \lambda v) dx; \quad \text{and} \\ &= \frac{\mu}{2} \int_{\Omega} |\nabla u|^2 dx - \int_{\Omega} f u dx \\ \frac{J(u + \lambda v) - J(v)}{\lambda} &= \frac{\frac{\mu}{2} \int_{\Omega} (|\nabla(u + \lambda v)|^2 - |\nabla u|^2) dx - \int_{\Omega} f(\lambda v) dx}{\lambda} \end{aligned} \quad (2.8)$$

using the definition; $|\vec{x}|^2 = \vec{x}^T \vec{x}$, we see that:

$$\begin{aligned} |(\nabla u + \lambda \nabla v)|^2 &= (\nabla u + \lambda \nabla v)^T (\nabla u + \lambda \nabla v) \\ &= (\nabla u)^T \nabla u + \lambda (\nabla u)^T \nabla v + \lambda (\nabla v)^T \nabla u + \lambda^2 (\nabla v)^T \nabla v \\ &= |\nabla u|^2 + \lambda (\nabla u)^T \nabla v + \lambda (\nabla v)^T \nabla u + \lambda^2 |\nabla v|^2 \end{aligned}$$

and;

$$\begin{aligned} \frac{|(\nabla u + \lambda \nabla v)|^2 - |\nabla u|^2}{\lambda} &= \frac{\lambda (\nabla u)^T \nabla v + \lambda (\nabla v)^T \nabla u + \lambda^2 |\nabla v|^2}{\lambda} \\ &= (\nabla u)^T \nabla v + (\nabla v)^T \nabla u + \lambda |\nabla v|^2 \\ &= 2(\nabla u)^T \nabla v + \lambda |\nabla v|^2 \end{aligned}$$

substituting this value into equation [2.8](#) yields;

$$\begin{aligned} \frac{J(u + \lambda v) - J(v)}{\lambda} &= \frac{\frac{\mu}{2} \int_{\Omega} (|\nabla(u + \lambda v)|^2 - |\nabla u|^2) dx}{\lambda} - \frac{\lambda \int_{\Omega} f v dx}{\lambda} \\ &= \frac{\mu}{2} \int_{\Omega} (2(\nabla u)^T \nabla v + \lambda |\nabla v|^2) dx - \int_{\Omega} f v dx \end{aligned}$$

now letting $\lambda \rightarrow 0$ we see that;

$$\frac{J(u + \lambda v) - J(v)}{\lambda} \rightarrow \frac{\mu}{2} \int_{\Omega} 2(\nabla u)^T \nabla v dx - \int_{\Omega} f v dx$$

Thus;

$$\mu \int_{\Omega} (\nabla u)^T \nabla v dx - \int_{\Omega} f v dx = 0. \quad (2.9)$$

In order to show the third part we make use of The Green's Theorem [11](#), Thus, let us assume that $f \in C(\Omega)$ and the solution $u \in H_0^1(\Omega)$ of [2.7](#) has the regularity property $u \in C^2(\Omega) \cap C_0(\bar{\Omega})$. Then by Green's formula;

$$\int_{\Omega} \nabla u \cdot \nabla v dx = - \int_{\Omega} \Delta u v dx + \int_{\Gamma} \frac{\partial u}{\partial n} v d\sigma$$

where $n := (n_1, n_2)^{\top}$ is the exterior unit normal vector. Thus equation [2.9](#) can be written as;

$$\int_{\Omega} (-\mu \Delta u - f) v dx = 0 \quad ; \forall v \in H_0^1(\Omega) \quad (2.10)$$

Since [2.10](#) holds true $\forall v \in H_0^1(\Omega)$, we conclude that ;

$$-\mu \Delta u(x) = f(x) \quad , f.f.a. \quad x \in \Omega$$

and by continuity, we find that u satisfies the boundary value problem ;

$$-\mu \Delta u(x) = f(x) \quad , \forall x \in \Omega \quad (2.11)$$

$$u(x) = 0 \quad x \in \Gamma \quad (2.12)$$

□

Optimality Condition: Let Ω be a bounded polygonal domain and $f \in L^2(\Omega)$.

The optimality condition;

$$\int_{\Omega} \nabla u \cdot \nabla v \, dx = \int_{\Omega} f v \, dx \quad \forall v \in H_0^1(\Omega)$$

can be expressed as;

$$\int_{\Omega} \nabla u \cdot \nabla v \, dx = - \int_{\Omega} \Delta u v \, dx \quad \forall v \in H_0^1(\Omega)$$

thanks to integration by parts and zero boundary condition.

Consequently;

$$-\Delta u = f \quad \text{in } \Omega \quad (2.13)$$

$$u = 0 \quad \text{on } \partial\Omega \quad (2.14)$$

We begin with the weak form of equation (2.2) and thus seek a $u \in H_0^1(\Omega)$ such that;

$$a(u, v) = F(v) \quad \forall v \in H_0^1(\Omega) \quad (2.15)$$

where the bilinear form $a(\cdot, \cdot)$ is defined as;

$$a(w, v) = \int_{\Omega} \nabla w \cdot \nabla v \, dx \quad \forall w, v \in H_0^1(\Omega)$$

and the linear functional $F(\cdot)$ is defined as;

$$F(v) = \int_{\Omega} f v \, dx \quad \forall v \in H_0^1(\Omega).$$

Below we show that $a(w, v)$ is a bilinear form.

Proof. Let $u, w, v \in H_0^1(\Omega)$. Then $a(\cdot, \cdot)$ defines a bilinear form because it satisfies:

1. $a(w, v) = \int_{\Omega} \nabla w \cdot \nabla v \, dx = \int_{\Omega} \nabla v \cdot \nabla w \, dx = a(v, w)$.
2. $a(w, w) = \int_{\Omega} \nabla w \cdot \nabla w \, dx \geq 0$ since $\nabla w \cdot \nabla w \geq 0$ and so;
 $a(w, w) = 0$ if and only if $\int_{\Omega} \nabla w \cdot \nabla w \, dx = 0$ this implies that $w = 0$

$$\begin{aligned}
3. \quad a(u + \lambda w, v) &= \int_{\Omega} \nabla(u + \lambda w) \cdot \nabla v \, dx \\
&= \int_{\Omega} \nabla u \cdot \nabla v \, dx + \lambda \int_{\Omega} \nabla w \cdot \nabla v \, dx \\
&= a(u, v) + \lambda a(w, v)
\end{aligned}$$

□

Next, we show that $F(\cdot)$ is a linear functional.

Proof. Let $u, v \in H_0^1(\Omega)$

$$\begin{aligned}
1. \quad \text{i.} \quad F(u + v) &= \int_{\Omega} f(u + v) \, dx \\
&= \int_{\Omega} (fu + fv) \, dx \\
&= \int_{\Omega} fu \, dx + \int_{\Omega} fv \, dx \\
&= F(u) + F(v)
\end{aligned}$$

$$\begin{aligned}
2. \quad \text{ii.} \quad F(\lambda v) &= \int_{\Omega} f(\lambda v) \, dx \\
&= \lambda \int_{\Omega} fv \, dx \\
&= \lambda F(v)
\end{aligned}$$

□

Therefore, F is a linear functional.

2.4 The Finite Element Method

In general, it is difficult to access the solution to the variational equation [2.15](#) analytically.

We therefore resort to using numerical methods where we seek an approximate solution in a suitable finite dimensional subspace $H_* \subset H_0^1(\Omega)$:

Find $u_h \in H_*$ such that;

$$a(u_h, v_h) = F(v_h) \quad v_h \in H_* \tag{2.16}$$

Since $a(\cdot, \cdot)$ is a bounded, $H_0^1(\Omega)$ -elliptic bilinear form, then the Lax Milgram Lemma guarantees that 2.5 admits a unique solution $u_h \in H_*$. Now, the choice of H_* will reflect on two

important factors namely:

- **Construction** of H_* such that the linear algebraic system represented by (2.16) can be solved efficiently.
- **Estimation** of the **global discretization error** $(u - u_h)$.

We pick a proper selection of a basis of H_* :

$$H_* = \text{span}\{\varphi_1, \varphi_2, \dots, \varphi_{n_h}\} \quad \text{thus} \quad \dim H_* = n_h \quad (2.17)$$

since the solution $u_h \in H_*$, it can be written as a linear combination of the basis functions and so;

$$u_h = \sum_{j=1}^{n_h} \alpha_j \varphi_j \quad (2.18)$$

Obviously, 2.5 holds for any $v_h \in H_*$ if and only if it holds true for all basis functions φ_i ; for $1 \leq i \leq n_h$. Therefore substituting 2.6 into 2.5 and choosing $v_h = \varphi_i$, $i = 1, 2, \dots, n_h$, we get that 2.5 corresponds to the linear algebraic system below;

$$\sum_{j=1}^{n_h} a(\varphi_j, \varphi_i) \alpha_j = F(\varphi_i) \quad , \quad 1 \leq i \leq n_h \quad (2.19)$$

From applications in structural mechanics, we define the **Stiffness Matrix and Load Vector**.

The matrix $A_h = (a_{ij})_{i,j=1}^{n_h}$ with entries;

$$a_{ij} := a(\varphi_j, \varphi_i) \quad , \quad 1 \leq i, j \leq n_h \quad (2.20)$$

That is;

$$\begin{pmatrix} a(\varphi_1, \varphi_1) & a(\varphi_2, \varphi_1) & \dots & a(\varphi_{n_h}, \varphi_1) \\ a(\varphi_2, \varphi_1) & a(\varphi_2, \varphi_2) & \dots & a(\varphi_{n_h}, \varphi_2) \\ \cdot & \cdot & \dots & \cdot \\ \cdot & \cdot & \dots & \cdot \\ \cdot & \cdot & \dots & \cdot \\ a(\varphi_{n_h}, \varphi_1) & a(\varphi_{n_h}, \varphi_2) & \dots & a(\varphi_{n_h}, \varphi_{n_h}) \end{pmatrix} \begin{pmatrix} \alpha_1 \\ \alpha_2 \\ \cdot \\ \cdot \\ \cdot \\ \alpha_{n_h} \end{pmatrix} = \begin{pmatrix} F(\varphi_1) \\ F(\varphi_2) \\ \cdot \\ \cdot \\ \cdot \\ F(\varphi_{n_h}) \end{pmatrix}$$

where the $F(\varphi_i)$, $1 \leq i \leq n_h$ is the load vector and A_h is the **stiffness matrix**.

Properties of A_h : Banded Matrix

The matrix $A_h = (a_{ij})_{i,j=1}^{n_h}$ with entries;

- $a_{ij} := a(\varphi_j, \varphi_i)$, $1 \leq i, j \leq n_h$ is called the **stiffness matrix** and the vector;
 $b_h = (b_1, b_2, \dots, b_{n_h})^T$ with components;
- $b_i := l(\varphi_i)$, $1 \leq i \leq n_h$

is referred to as the **load vector**.

The unknowns in the first part are the coefficients α_i , $1 \leq i \leq n_h$ which constitute the solution vector $\alpha_h = (\alpha_1, \alpha_2, \dots, \alpha_{n_h})^T$. In summary, the linear algebraic system can be concisely written as;

$$A_h \alpha_h = b_h \tag{2.21}$$

2.4.1 Importance of the Finite Element Method

The Finite Element Method (FEM) has the following advantages:

1. **Modeling:** FEM makes modeling of complex geometrical and irregular shapes easier and achievable. Here, both interior and exterior parts of these shapes can be modeled and the mathematician predicts or determines how critical factors might affect the entire structure and why failures might occur.
2. **Visualization:** Engineers can easily spot any vulnerability in design with the detailed visualizations FEM produces, then use the new data to make a new design.
3. **Accuracy:** While modeling a complex physical deformity by hand can be impractical, a computer using FEM can solve the problem with a high degree of accuracy.

4. **Time-dependent simulation:** FEM is highly useful for certain time dependent simulations, such as crash simulations, in which deformations in one area depend on deformation in another area.
5. **Boundaries:** With FEM, designers can use boundary conditions to define to which conditions the model needs to respond. Boundary conditions can include point forces, distributed forces, thermal effects (such as temperature changes or applied heat energy), and positional constraints.
6. **Adaptability:** FEM can be adapted to meet certain specifications for accuracy in order to decrease the need for physical prototypes in the design process. Creating multiple iterations of initial prototypes is usually a costly and timely process. Instead of spending weeks on hard prototyping, the designer can model different designs and materials in hours via software.

In the Finite Element Method, we:

- Obtain the weak formulation of the equation which is also called the Variational statement.
- Choose approximations for unknown functions which in our case are displacements.
- Solve the current equation(s) augmented with boundary values.

Numerical Experiments

Under the Finite Element Numerical Method, the approximate solution to 2.2 is gotten through Fenics. Thus, a bunch of experiments are done for different values of the step size $h = \frac{1}{N}$, errors at each 'N' for norms L^2 and H^1 , corresponding maximum errors and convergence rates.

Experiment 1

This first example is a FEniCS tutorial demo program called ‘**assignment-poisson.py**’: Poisson equation with Dirichlet boundary conditions. Test problem is chosen to give an exact solution at all nodes of the mesh.

$$\begin{aligned}
 -\Delta u &= f \text{ in } \Omega = (0, 1)^2 \\
 u &= u_D \text{ on the boundary} \\
 u_D &= 1 + x^2 + 2y^2 \\
 f &= -6
 \end{aligned}$$

The mesh was created for each n starting with; `mesh = UnitSquareMesh(8, 8)` and the function space defined as; `V = FunctionSpace(mesh, ‘P’ , 1)`.

The Numerical Analysis carried out yielded the table below;

Table 2.2: Numerical Simulations

Numerical Results for polynomial of degree 2				
$h = \frac{1}{N}$	Error in L2	Error in H1	Maximum Error	Convergence Rate (r) or Order in L2
$\frac{1}{8}$	8.2351×10^{-3}	1.6158×10^{-1}	$1.3323 \exp^{-15}$	—
$\frac{1}{16}$	2.0588×10^{-3}	8.0713×10^{-2}	$5.7732 \exp^{-15}$	2.0001
$\frac{1}{32}$	5.2469×10^{-4}	4.0347×10^{-2}	$2.2204 \exp^{-14}$	1.9724
$\frac{1}{64}$	1.2867×10^{-4}	2.1722×10^{-2}	$1.0436 \exp^{-13}$	2.0280
$\frac{1}{128}$	3.2168×10^{-5}	1.0086×10^{-2}	$4.5053 \exp^{-13}$	2.0001
$\frac{1}{256}$	8.0420×10^{-6}	5.0430×10^{-3}	$1.8863 \exp^{-12}$	2.0001
$\frac{1}{512}$	2.0105×10^{-6}	2.5215×10^{-3}	$7.6514 \exp^{-12}$	2.0001

Convergence Rate

For finite element methods, this typically corresponds to proving, theoretically or empirically, that the error $e = u_e - u$ is bounded by the mesh size h to some power r ; that is, $\|e\| \leq Ch^r$ for some constant $C \in \mathbb{R}$. The number r is called the convergence rate of the method. Note that different norms, like the L2-norm $\|e\|$ or H1-norm $\|\nabla e\|$ typically have different convergence rates.

In computing these convergence rates, we first define the element size $h = \frac{1}{N}$, where N is the number of cell divisions in the x and y directions. We perform experiments with $h_0 > h_1 > h_2 \dots$ and compute the corresponding errors $E_0, E_1, E_2 \dots$ as indicated above. Assuming $E_i = Ch_i^r$ for these unknown constants C and r , we can compare two consecutive experiments, $E_{i-1} = Ch_{i-1}^r$ and $E_i = Ch_i^r$, and solve for r :

$$r = \frac{\text{Log}(E_i/E_{i-1})}{\text{Log}(h_i/h_{i-1})}$$

The r values should approach the expected convergence rate as i increases.

Chapter 3

A C^0 Interior Penalty Finite Element Method

This chapter describes the spatial discretization of the fourth order term involving the operator Δ^2 which appears in (4.6a)-(4.6b). To simplify, we present the spatial discretization for the following biharmonic equation augmented with Cahn-Hilliard type boundary conditions.

$$\Delta^2 u(\mathbf{x}) + u(\mathbf{x}) = f(\mathbf{x}) \quad \forall \mathbf{x} \in \Omega, \quad (3.1)$$

$$\frac{\partial u(\mathbf{x})}{\partial \mathbf{n}} = \frac{\partial \Delta u(\mathbf{x})}{\partial \mathbf{n}} = 0 \quad \forall \mathbf{x} \in \partial\Omega. \quad (3.2)$$

The fundamental challenge with the equation is that it takes four derivatives of the solution. In the case of the Laplace equation seen in 2.13,

But for the biharmonic equation, if one followed the same procedure using the test and trial functions that work for the weak form of the Laplace equation, these test and trial functions contain insufficient regularity to support the integration by parts performed twice over Ω . Instead, if one were to partition $\Omega = \bigcup_{K \in \mathcal{T}_h} K$ and use the usual globally continuous, cellwise polynomial functions with their kinks on the cell interfaces, say $v, w \in C^\infty(\bar{K})$ where $K \in \mathcal{T}_h$. This allows us to perform the integration by parts twice in the following

manner:

$$\begin{aligned}
 \int_K v(\Delta^2 w) \, dx &= \int_{\partial K} v \frac{\partial \Delta w}{\partial \mathbf{n}} \, ds - \int_K \nabla v \cdot \nabla(\Delta w) \, dx \\
 &= \int_{\partial K} v \frac{\partial \Delta w}{\partial \mathbf{n}} \, ds - \int_{\partial K} \nabla v \cdot \frac{\partial \nabla w}{\partial \mathbf{n}} \, dx \\
 &\quad + \int_K D^2 v : D^2 w \, dx.
 \end{aligned}$$

When we sum over all cells $K \in \mathcal{T}_h$, we end up with multi-valued gradient and third order derivative on each interface shared by K_+ and K_- .

3.0.1 History of the C^0 IP method

The C^0 IP methods became very attractive in the recent past for approximating the solutions of higher order problems like the Biharmonic equation. Since a natural idea is to use finite elements that are “ C^1 continuous”, i.e., that use shape functions which are not just continuous but also have continuous first derivatives. An example of such an element is the Argyris element developed in the late 1960s. However, owing to their computational cost, have been seldom used. Another approach is to consider mixed methods however this results in a saddle point problem and hence an indefinite system. The approach followed in this thesis relies on using continuous (but not C^1 continuous) shape functions and penalize the jump in the derivative to obtain a scheme for an equation that has two derivatives on each shape function. In analogy to the Interior Penalty (IP) method for the Laplace equation, this scheme for the biharmonic equation is typically called the C^0 IP method, since it uses C^0 (continuous but not continuously differentiable) shape functions with an interior penalty.

3.0.2 Derivation of the C^0 IP method

This method relies on the use of C^0 Lagrange finite elements where the C^1 continuity requirement is relaxed and has been replaced with interior penalty techniques. To derive

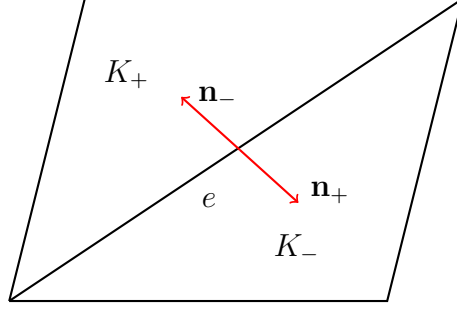


Figure 3.1: Orientation of the unit normal, tangent to the interface e shared by the cells K_- and K_+ in 2D.

this method, we consider a C^0 shape function v_h which vanishes on $\partial\Omega$. Since the higher order derivatives of v_h have two values on each interface $e \in \mathbb{E}_h$ (shared by the two cells $K_+, K_- \in \mathcal{T}_h$), we cope with this discontinuity by defining the following single-valued functions on e :

$$\begin{aligned} \left[\left[\frac{\partial^k v_h}{\partial \mathbf{n}^k} \right] \right] &= \frac{\partial^k v_h|_{K_+}}{\partial \mathbf{n}^k} \Big|_e - \frac{\partial^k v_h|_{K_-}}{\partial \mathbf{n}^k} \Big|_e, \\ \left\{ \left\{ \frac{\partial^k v_h}{\partial \mathbf{n}^k} \right\} \right\} &= \frac{1}{2} \left(\frac{\partial^k v_h|_{K_+}}{\partial \mathbf{n}^k} \Big|_e + \frac{\partial^k v_h|_{K_-}}{\partial \mathbf{n}^k} \Big|_e \right) \end{aligned}$$

for $k = 1, 2$ (i.e., for the gradient and the matrix of second derivatives), and where \mathbf{n} denotes a unit vector normal to e pointing from K_+ to K_- (cf. Figure 1 below). In the literature, these functions are referred to as the “jump” and “average” operations, respectively. To obtain the C^0 IP approximation u_h , we left multiply the biharmonic equation by v_h , integrate and apply the following integration-by-parts formula on each mesh cell $K \in \mathcal{T}_h$:

$$\begin{aligned} \int_K (\Delta^2 w) v \, dx &= \int_{\partial K} \frac{\partial \Delta w}{\partial \mathbf{n}} v \, ds - \int_{\partial K} \frac{\partial^2 w}{\partial \mathbf{n} \partial \mathbf{t}} \frac{\partial v}{\partial \mathbf{t}} \, ds - \int_{\partial K} \frac{\partial^2 w}{\partial \mathbf{n}^2} \frac{\partial v}{\partial \mathbf{n}} \, ds \\ &\quad + \int_K D^2 w : D^2 v \, dx, \end{aligned}$$

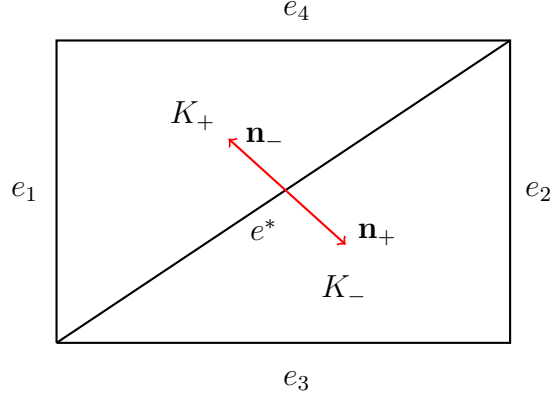


Figure 3.2: Representation of two cells K_- and K_+ in 2D having a shared edge e^* and boundary edges e_1 , e_2 , e_3 , and e_4

where \mathbf{t} is the counterclockwise tangent and $D^2v : D^2w$ is the Frobenius inner product of Hessian matrices of v and w , $\frac{\partial}{\partial n}$ and $\frac{\partial}{\partial t}$ denote the exterior normal derivative and the counterclockwise tangential derivative. Then, summing over all the cells or triangles $K \in \mathcal{T}_h$, with $w = u$ and after like cancellations, we get;

$$\sum_{K \in \mathcal{T}_h} \int_K (\Delta^2 u) v dx = - \sum_{K \in \mathcal{T}_h} \int_{\partial K} \left(\frac{\partial^2 u}{\partial n^2} \right) \left(\frac{\partial v}{\partial n} \right) ds + \sum_{K \in \mathcal{T}_h} \int_K D^2 u : D^2 v dx \quad (3.3)$$

Take for example, the edges and shared edge between two cells in the diagram below; Rewriting the first term in the right hand side of [3.3](#) as a sum over the edges in \mathbb{E}_h , we get:

$$- \sum_{K \in \mathcal{T}_h} \int_{\partial K} \left(\frac{\partial^2 u}{\partial n^2} \right) \left(\frac{\partial v}{\partial n} \right) ds = \int_{e^*} \left(\frac{\partial^2 u_1}{\partial n_1^2} \frac{\partial v_1}{\partial n_1} \right) ds + \underbrace{\int_{e_1 \cup e_2 \cup e_3 \cup e_4} \left(\frac{\partial^2 u}{\partial n^2} \frac{\partial v}{\partial n} \right) ds}_{\text{this term equals zero}} \quad (3.4)$$

$$+ \int_{e^*} \left(\frac{\partial^2 u_k}{\partial n_4^2} \frac{\partial v_k}{\partial n_4} \right) ds \quad (3.5)$$

where u_1, u_2, u_3, u_k are the restrictions of u on K_1, K_2, K_3, K_4 likewise v_1, v_2, v_3, v_4 , e^* represents the common edge shared by cells, e_1, e_2, e_3, e_4 which are boundary edges. Conse-

quently, we require single valued function for $\frac{\partial^2 u}{\partial n^2}$ and $\frac{\partial v}{\partial n}$ on $e \equiv e^*$ for edge e , thus we fix $n = n_e = n_1 = -n_2$. Note that n_1 and n_2 are replaced interchangeably with n_+ and n_- . Now according to the figure above, equation [3.4](#) becomes:

$$-\sum_{K \in \mathcal{T}_h} \int_{\partial K} \left(\frac{\partial^2 u}{\partial n^2} \right) \left(\frac{\partial v}{\partial n} \right) ds = \int_{e^*} \left(\frac{\partial^2 u_1}{\partial n_+^2} \frac{\partial v_1}{\partial n_+} + \frac{\partial^2 u_2}{\partial n_-^2} \frac{\partial v_2}{\partial n_-} \right) ds \quad (3.6)$$

$$= \int_e \frac{\partial^2 u}{\partial n_e^2} \left(\frac{\partial v_1}{\partial n_+} + \frac{\partial v_2}{\partial n_-} \right) ds \quad (3.7)$$

$$= \int_e \frac{\partial^2 u}{\partial n_e^2} \left(\frac{\partial v_1}{\partial n_+} - \frac{\partial v_2}{\partial n_+} \right) ds \quad (3.8)$$

Here, $n_1 = -n_2$ or $n_+ = -n_-$ e.t.c. We then arrive at this equation;

$$-\sum_{K \in \mathcal{T}_h} \int_{\partial K} \left(\frac{\partial^2 u}{\partial n^2} \right) \left(\frac{\partial v}{\partial n} \right) ds = \sum_{e \in \mathbb{E}_h} \int_e \left(\frac{\partial^2 u}{\partial n_e^2} \right) \left[\left[\frac{\partial v}{\partial n_e} \right] \right] ds \quad (3.9)$$

where n_e is a unit vector normal to the edge e and the jump $\left[\left[\frac{\partial v}{\partial n_e} \right] \right]$ is defined as follows. Note that the negative sign in [3.9](#) is absorbed due to the choice of n_1 or n_2 e.t.c. Thus, for an interior edge shared by two cells K_{\pm} where n_e points from K_- to K_+ , we define the jump on this edge as;

$$\left[\left[\frac{\partial v}{\partial n_e} \right] \right] = n_e \cdot (\nabla v_+ - \nabla v_-) \quad (3.10)$$

and;

$$\frac{\partial^2 u}{\partial n_e^2} = n_e \cdot (\nabla^2 u) n_e \quad (3.11)$$

for a boundary edge, the jump is defined as;

$$\left[\left[\frac{\partial v}{\partial n_e} \right] \right] = -n_e \cdot (\nabla v_K) \quad (3.12)$$

and [3.11](#) remains the same.

combining equations [3.3](#) to [3.9](#) together with the right hand side of the model problem [3.1](#),

we arrive at;

$$\sum_{K \in \mathcal{T}_h} \int_K D^2 u : D^2 v \, dx + \sum_{e \in \mathbb{E}_h} \int_e \left(\frac{\partial^2 u}{\partial n_e^2} \right) \left[\left[\frac{\partial v}{\partial n_e} \right] \right] ds = \int_{\Omega} f v \, dx \quad \forall v \in V_h \quad (3.13)$$

Since $\frac{\partial^2 u}{\partial n_e^2}$ has the same trace from either side of the edge e , it can be re-written as;

$$\frac{\partial^2 u}{\partial n_e^2} = \left\{ \left\{ \frac{\partial^2 u}{\partial n_e^2} \right\} \right\}$$

Recall that $u \in H^4(\Omega)$ satisfies [3.1](#), thus the average of the second order normal derivative from the two sides of the edge e is defined on an interior edge as;

$$\frac{\partial^2 u}{\partial n_e^2} = \frac{1}{2} \left(\frac{\partial^2 u_-}{\partial n_e^2} + \frac{\partial^2 u_+}{\partial n_e^2} \right) = \left\{ \left\{ \frac{\partial^2 u}{\partial n_e^2} \right\} \right\}$$

and on a boundary edge as;

$$\frac{\partial^2 u}{\partial n_e^2} = \frac{\partial^2 u_K}{\partial n_e^2} = \left\{ \left\{ \frac{\partial^2 u}{\partial n_e^2} \right\} \right\}$$

[3.13](#) becomes;

$$\sum_{K \in \mathcal{T}_h} \int_K D^2 u : D^2 v \, dx + \sum_{e \in \mathbb{E}_h} \int_e \left\{ \left\{ \frac{\partial^2 u}{\partial n_e^2} \right\} \right\} \left[\left[\frac{\partial v}{\partial n_e} \right] \right] ds = \int_{\Omega} f v \, dx \quad \forall v \in V_h \quad (3.14)$$

Observe that the first term at the left hand side of [3.14](#) is symmetric as should be but the second term is not since its symmetric equivalent $\left[\left[\frac{\partial u}{\partial n_e} \right] \right] = 0 \quad \forall e \in \mathbb{E}_h$. Due to this, we introduce this symmetric equivalent as an extra term which does not change anything at all. We get;

$$\sum_{K \in \mathcal{T}_h} \int_K D^2 u : D^2 v \, dx + \sum_{e \in \mathbb{E}_h} \int_e \left\{ \left\{ \frac{\partial^2 u}{\partial n_e^2} \right\} \right\} \left[\left[\frac{\partial v}{\partial n_e} \right] \right] ds \quad (3.15)$$

$$+ \sum_{e \in \mathbb{E}_h} \int_e \left\{ \left\{ \frac{\partial^2 v}{\partial n_e^2} \right\} \right\} \left[\left[\frac{\partial u}{\partial n_e} \right] \right] ds = \int_{\Omega} f v \, dx \quad \forall v \in V_h \quad (3.16)$$

This has better properties due to the inclusion of the symmetric term since [3.15](#) is not coercive; a property crucial for well-posedness. (note that [3.15](#) has to satisfy Lax Milgram's Theorem to ensure the availability of a solution to the linear system). This is done by

including a stability term to the equation which balances everything out. We then arrive finally at the last equation;

$$\sum_{K \in \mathcal{T}_h} \int_K D^2 u : D^2 v \, dx + \sum_{e \in \mathbb{E}_h} \int_e \left\{ \left\{ \frac{\partial^2 u}{\partial n_e^2} \right\} \right\} \left[\left[\frac{\partial v}{\partial n_e} \right] \right] ds \quad (3.17)$$

$$+ \sum_{e \in \mathbb{E}_h} \int_e \left\{ \left\{ \frac{\partial^2 v}{\partial n_e^2} \right\} \right\} \left[\left[\frac{\partial u}{\partial n_e} \right] \right] ds + \sum_{e \in \mathbb{E}_h} \frac{\alpha}{h_e} \int_e \left[\left[\frac{\partial u}{\partial n_e} \right] \right] \left[\left[\frac{\partial v}{\partial n_e} \right] \right] ds \quad (3.18)$$

$$= \int_{\Omega} f v \, dx \quad \forall v \in V_h \quad (3.19)$$

where $\alpha > 0$ is a penalty parameter of choice and h_e is the length of an edge $e \in \mathbb{E}_h$

We now formulate the C^0 interior penalty method for [3.1](#) as follows;

Find $u_h \in V_h$ such that:

$$\mathcal{A}_h(u_h, v) = \mathcal{F}(v) \quad \text{holds for all test functions } v \in V_h \quad (3.20)$$

where the bilinear form $\mathcal{A}_h(u_h, v)$ defined on the piecewise Sobolev space $H^3(\Omega, \mathcal{T}_h)$ is expressed as;

$$\mathcal{A}_h(u_h, v) := \sum_{K \in \mathcal{T}_h} \int_K D^2 u_h : D^2 v \, dx + \sum_{e \in \mathbb{E}_h} \int_e \left\{ \left\{ \frac{\partial^2 u_h}{\partial n_e^2} \right\} \right\} \left[\left[\frac{\partial v}{\partial n_e} \right] \right] ds \quad (3.21)$$

$$+ \sum_{e \in \mathbb{E}_h} \int_e \left\{ \left\{ \frac{\partial^2 v}{\partial n_e^2} \right\} \right\} \left[\left[\frac{\partial u_h}{\partial n_e} \right] \right] ds + \sum_{e \in \mathbb{E}_h} \frac{\alpha}{h_e} \int_e \left[\left[\frac{\partial u_h}{\partial n_e} \right] \right] \left[\left[\frac{\partial v}{\partial n_e} \right] \right] ds \quad (3.22)$$

$$= \int_{\Omega} f v \, dx \quad \forall v \in V_h \quad (3.23)$$

and

$$\mathcal{F}(v) := \sum_{K \in \mathcal{T}_h} \int_K f v \, dx + \sum_{e \in \mathbb{E}_h} \frac{\alpha}{h_e} \int_e \frac{\partial v}{\partial n_e} j \, ds. \quad (3.24)$$

Note that ;

$$D^2 u : D^2 v = \sum_{i,j}^2 u_{x_i x_j} v_{x_i x_j}. \quad (3.25)$$

Thus;

For all $u_h \in H^2(\Omega, \mathcal{T}_h)$ and $v \in V_h$ such that u_h vanishes at all the vertices of \mathcal{T}_h . Then, we sum up all $K \in \mathcal{T}_h$, then by integration by parts and using the equality $ab+cd = \frac{(a+c)(b+d)}{2} + \frac{(a-c)(b-d)}{2}$, we get

$$\begin{aligned} \sum_{K \in \mathcal{T}_h} \int_K D^2 u_h : D^2 v dx &= \sum_{K \in \mathcal{T}_h} \int_{\partial K} \left(\frac{\partial^2 u_h}{\partial n^2} \frac{\partial v}{\partial n} + \frac{\partial^2 u_h}{\partial t \partial n} \frac{\partial v}{\partial t} \right) ds \\ &= - \sum_{e \in \mathbb{E}_h} \int_e \left\{ \left\{ \frac{\partial^2 u_h}{\partial n^2} \right\} \right\} \left[\left[\frac{\partial v}{\partial n} \right] \right] ds - \sum_{e \in \mathbb{E}_h^i} \int_e \left\{ \left\{ \frac{\partial v}{\partial n} \right\} \right\} \left[\left[\frac{\partial^2 u_h}{\partial n^2} \right] \right] ds \end{aligned} \quad (3.26)$$

Now, we define $\|\cdot\|_h$,

$$\|v\|_h^2 = a_h(v, v) + \sum_{e \in \mathbb{E}_h} \frac{\alpha}{h_e} \int_e \left[\left[\frac{\partial v}{\partial n} \right] \right]^2 ds \quad \forall v \in H^2(\Omega, \mathcal{T}_h) \quad (3.27)$$

where the bilinear form $a_h(\cdot, \cdot)$ is defined by,

$$a_h(u, v) = \sum_{K \in \mathcal{T}_h} \int_K D^2 u : D^2 v dx \quad \forall v, u \in H^2(\Omega, \mathcal{T}_h) \quad (3.28)$$

Now, $|\cdot|_{a_h}$ is the seminorm corresponding to $a_h(\cdot, \cdot)$, i.e.

$$\begin{aligned} |v|_{a_h}^2 &= a_h(v, v) = \sum_{K \in \mathcal{T}_h} \int_K D^2 v : D^2 v dx = \sum_{K \in \mathcal{T}_h} |v|_{H^2(K)}^2 \\ |v|_{a_h} &= |v|_{H^2(\Omega)} \quad \forall v \in H^2(\Omega) \end{aligned}$$

□

3.0.3 Continuity of $A_h(u_h, v_h)$

Theorem:

There exists a constant $C_1 > 0$ which depends only on the shape regularity of \mathcal{T}_h such that

$$\forall u_h, v_h \in V_h \quad |A_h(u_h, v_h)| \leq C_1 \|u_h\|_h \|v_h\|_h \quad (3.29)$$

Proof. From (3.21) we know,

$$\begin{aligned}
\mathcal{A}_h(u_h, v_h) &:= \sum_{K \in \mathcal{T}_h} \int_K D^2 u_h : D^2 v_h \, dx + \sum_{e \in \mathbb{E}_h} \int_e \left\{ \left\{ \frac{\partial^2 u_h}{\partial n_e^2} \right\} \right\} \left[\left[\frac{\partial v_h}{\partial n_e} \right] \right] ds \\
&+ \sum_{e \in \mathbb{E}_h} \int_e \left\{ \left\{ \frac{\partial^2 v_h}{\partial n_e^2} \right\} \right\} \left[\left[\frac{\partial u_h}{\partial n_e} \right] \right] ds + \sum_{e \in \mathbb{E}_h} \frac{\alpha}{h_e} \int_e \left[\left[\frac{\partial u_h}{\partial n_e} \right] \right] \left[\left[\frac{\partial v_h}{\partial n_e} \right] \right] ds \\
&= \mathfrak{E}_1 + \mathfrak{E}_2 + \mathfrak{E}_3 + \mathfrak{E}_4
\end{aligned} \tag{3.30}$$

Now, by using Cauchy-Schwarz inequality we get,

$$\begin{aligned}
|\mathfrak{E}_1| &= \left| \int_K D^2 u_h : D^2 v_h \, dx \right| \leq \left(\int_K |D^2 u_h|^2 \right)^{1/2} \left(\int_K |D^2 v_h|^2 \right)^{1/2} \\
&\leq \|u_h\|_h \|v_h\|_h
\end{aligned} \tag{3.31}$$

Then, implementing the trace inequality and standard inverse estimate for the symmetry terms $\mathfrak{E}_2, \mathfrak{E}_3$, we arrive at;

$$\begin{aligned}
|\mathfrak{E}_2| &= \sum_{e \in \mathbb{E}_h} \left| \int_e \left\{ \left\{ \frac{\partial^2 u_h}{\partial n_e^2} \right\} \right\} \left[\left[\frac{\partial v_h}{\partial n_e} \right] \right] ds \right| \leq \left(\sum_{e \in \mathbb{E}_h} |h_e| \left\| \left\{ \left\{ \frac{\partial^2 u_h}{\partial n_e^2} \right\} \right\} \right\|_{L^2(e)}^2 \right)^{\frac{1}{2}} \left(\sum_{e \in \mathbb{E}_h} |h_e|^{-1} \left\| \left[\left[\frac{\partial v_h}{\partial n_e} \right] \right] \right\|_{L^2(e)}^2 \right)^{\frac{1}{2}} \\
&\leq c^{\frac{1}{2}} \left(\sum_{e \in \mathbb{E}_h} \sum_{K \in \mathcal{T}_e} |u_h|_{H^2(K)}^2 \right) \left(\sum_{e \in \mathbb{E}_h} |h_e|^{-1} \left\| \left[\left[\frac{\partial v_h}{\partial n_e} \right] \right] \right\|_{L^2(e)}^2 \right)^{\frac{1}{2}} \\
&\leq c^{\frac{1}{2}} \left(\sum_{K \in \mathcal{T}_e} |u_h|_{H^2(K)}^2 \right) \left(\sum_{e \in \mathbb{E}_h} |h_e|^{-1} \left\| \left[\left[\frac{\partial v_h}{\partial n_e} \right] \right] \right\|_{L^2(e)}^2 \right)^{\frac{1}{2}} \\
&\leq c^{\frac{1}{2}} \|u_h\|_h \|v_h\|_h
\end{aligned} \tag{3.32}$$

Now, similarly for \mathfrak{E}_3 we get;

$$|\mathfrak{E}_3| = \sum_{e \in \mathbb{E}_h} \left| \int_e \left\{ \left\{ \frac{\partial^2 v_h}{\partial n_e^2} \right\} \right\} \left[\left[\frac{\partial u_h}{\partial n_e} \right] \right] ds \right| \leq c^{\frac{1}{2}} \|v_h\|_h \|u_h\|_h \tag{3.33}$$

For the last term \mathfrak{E}_4 , we apply the Cauchy-Schwarz inequality again to get;

$$\begin{aligned}
|\mathfrak{E}_4| &= \left| \sum_{e \in \mathbb{E}_h} \frac{\alpha}{h_e} \int_e \left[\left[\frac{\partial u_h}{\partial n_e} \right] \right] \left[\left[\frac{\partial v_h}{\partial n_e} \right] \right] ds \right| \\
&\leq \left(\sum_{e \in \mathbb{E}_h} \frac{\alpha}{h_e} \left\| \left[\left[\frac{\partial u_h}{\partial n_e} \right] \right] \right\|_{L^2(e)}^2 \right)^{1/2} \left(\sum_{e \in \mathbb{E}_h} \frac{\alpha}{h_e} \left\| \left[\left[\frac{\partial v_h}{\partial n_e} \right] \right] \right\|_{L^2(e)}^2 \right)^{1/2} \\
&\leq \|u_h\|_h \|v_h\|_h
\end{aligned} \tag{3.34}$$

Finally, collecting all from (3.31), (3.32), (3.33) and (3.34) we get;

$$|A_h(u_h, v_h)| \leq |\mathfrak{E}_1| + |\mathfrak{E}_2| + |\mathfrak{E}_3| + |\mathfrak{E}_4| \leq C_1 \|u_h\|_h \|v_h\|_h \quad \forall u_h, v_h \in V_h \tag{3.35}$$

where the mesh-dependent norm $\|\cdot\|_h$ is defined as;

$$\|v\|_h^2 = \sum_{K \in \mathcal{T}_h} |v|_{H^2(K)}^2 + \sum_{e \in \mathbb{E}_h} \frac{\alpha}{|h_e|} \left\| \left[\left[\frac{\partial v}{\partial n_e} \right] \right] \right\|_{L^2(e)}^2$$

□

3.0.4 Coercivity of $A_h(u_h, v_h)$

Theorem:

There exists a constant $C_\alpha > 0$ and $\alpha^* > 0$ which depends only on the shape regularity of \mathcal{T}_h such that if $\alpha > \alpha^*$, then;

$$\forall u_h, v_h \in V_h \quad A_h(u_h, u_h) \geq C_\alpha \|u_h\|_h^2 \tag{3.36}$$

Proof. $\forall u_h, v_h \in V_h$ from (3.21) we know,

$$\begin{aligned}
A_h(u_h, u_h) &= \int_K D^2 u_h : D^2 u_h \, dx + 2 \sum_{e \in \mathbb{E}_h^b} \int_e \left\{ \left\{ \frac{\partial^2 u_h}{\partial n_e^2} \right\} \right\} \left[\left[\frac{\partial u_h}{\partial n_e} \right] \right] ds + \sum_{e \in \mathbb{E}_h} \frac{\alpha}{h_e} \int_e \left[\left[\frac{\partial u_h}{\partial n_e} \right] \right]^2 ds \\
&= \sum_{K \in \mathcal{T}_h} |u_h|_{H^2(K)}^2 + 2 \sum_{e \in \mathbb{E}_h^b} \int_e \left\{ \left\{ \frac{\partial^2 u_h}{\partial n_e^2} \right\} \right\} \left[\left[\frac{\partial u_h}{\partial n_e} \right] \right] ds + \sum_{e \in \mathbb{E}_h} \frac{\alpha}{h_e} \int_e \left\| \left[\left[\frac{\partial u_h}{\partial n_e} \right] \right] \right\|_{L^2(e)}^2 ds
\end{aligned} \tag{3.37}$$

Now following (3.32) we get that,

$$\begin{aligned}
\left| \sum_{e \in \mathbb{E}_h^b} \int_e \left\{ \left\{ \frac{\partial^2 u_h}{\partial n_e^2} \right\} \right\} \left[\left[\frac{\partial u_h}{\partial n_e} \right] \right] ds \right| &\leq \left(\sum_{e \in \mathbb{E}_h} h_e \left\| \left\{ \left\{ \frac{\partial^2 u_h}{\partial n_e^2} \right\} \right\} \right\|_{L^2(e)}^2 \right)^{1/2} \left(\sum_{e \in \mathbb{E}_h} h_e^{-1} \left\| \left[\left[\frac{\partial u_h}{\partial n_e} \right] \right] \right\|_{L^2(e)}^2 \right)^{1/2} \\
&\leq (c)^{1/2} \sum_{K \in \mathcal{T}_h} |u_h|_{H^2(K)} \sum_{e \in \mathbb{E}_h} h_e^{-1/2} \left\| \left[\left[\frac{\partial u_h}{\partial n_e} \right] \right] \right\|_{L^2(e)}
\end{aligned} \tag{3.38}$$

Now,

$$\begin{aligned}
A_h(u_h, u_h) &\geq \sum_{K \in \mathcal{T}_h} |u_h|_{H^2(K)}^2 - 2(c)^{1/2} \sum_{K \in \mathcal{T}_h} |u_h|_{H^2(K)} \sum_{e \in \mathbb{E}_h} h_e^{-1/2} \left\| \left[\left[\frac{\partial u_h}{\partial n_e} \right] \right] \right\|_{L^2(e)} \\
&\quad + \sum_{e \in \mathbb{E}_h} \frac{\alpha}{h_e} \left\| \left[\left[\frac{\partial u_h}{\partial n_e} \right] \right] \right\|_{L^2(e)}^2
\end{aligned}$$

Now we use the following inequality, let β be a positive real number and $\alpha > \beta^2$ then for all $x, y \in \mathbb{R}$

$$x^2 - 2\beta xy + \alpha y^2 \geq \frac{\alpha - \beta^2}{1 + \alpha} (x^2 + y^2)$$

By applying this inequality with $\beta = 2(c)^{1/2}$, $x = |u_h|_{H^2(K)}$, $y = h_e^{-1/2} \left\| \left[\left[\frac{\partial u_h}{\partial n_e} \right] \right] \right\|_{L^2(e)}$

$$\begin{aligned}
A_h(u_h, u_h) &\geq \frac{\sum_{e \in \mathbb{E}_h} \frac{\alpha}{h_e} - \frac{4c}{h_e}}{1 + \sum_{e \in \mathbb{E}_h} \frac{\alpha}{h_e}} \left(\sum_{K \in \mathcal{T}_h} |u_h|_{H^2(K)}^2 + \sum_{e \in \mathbb{E}_h} h_e^{-1} \left\| \left[\left[\frac{\partial u_h}{\partial n_e} \right] \right] \right\|_{L^2(e)}^2 \right) \\
&= C_\alpha |u_h|_h
\end{aligned}$$

□

The continuity and coercivity of the bilinear form (3.21) guarantees a unique solution $u_h \in V_h$.

3.0.5 Quality of the Solutions

On polygonal domains, the weak solution u to the biharmonic equation lives in $H^{2+\alpha}(\Omega)$ where $\alpha \in (1/2, 2]$ is determined by the interior angles at the corners of Ω . For instance,

whenever Ω is convex, α is larger than 1 and α is close to 1 if one of the interior angles is close to π .

Convergence Rates

Suppose that the C^0 IP solution u_h is approximated by C^0 shape functions whose degree on each cell is at most $p \geq 2$.

Convergence in the C^0 IP-norm:

Assume that $f \in H^m(\Omega)$, $u \in H^k(\Omega)$ where $2 < k \leq m + 4$, $m \geq 0$. Then, the convergence rate of the C^0 IP method is $\mathcal{O}(h^{\min\{p-1, k-2\}})$ measured in the following mesh-dependent C^0 IP norm:

$$\|u_h\|_h^2 := \sum_{K \in \mathcal{T}_h} |u_h|_{H^2(K)}^2 + \alpha \sum_{e \in \mathbb{E}_h} h_e^{-1} \| [[\partial u_h / \partial \mathbf{n}]] \|_{L^2(e)}^2.$$

The optimal convergence rate $\mathcal{O}(h^{m+2})$ is achieved whenever $u \in H^{m+4}(\Omega)$ and p is chosen to be at least $m + 3$. This regularity assumption does not always guaranteed on polygonal domains however, is satisfied on smooth domains which do not contain angular corners.

Table 3.1: Operators and Function Spaces

Notations			
Chapters	S/No	Operators	Function Spaces
	1	h : mesh size	$C^\infty(\bar{\Omega})$: The space of infinitely differentiable functions on Ω .
Chapter 3	2	$\mathcal{T}_h = \{K_i : i = 1, 2, \dots, M\}$: triangulation of Ω for each K per mesh size.	
	3	\mathbb{E}_h : The set of all edges in \mathcal{T}_h .	
	4	K : non-overlapping triangles (finite elements).	
	5	$\bigcup_{K \in \mathcal{T}_h} K = \Omega$	
	6	$P_q(K)$: set of polynomials of degree $\leq q \in N$ on K .	
	7	$(D^2u : D^2v)$: Frobenius Inner Product of the Hessian Matrices of u and v .	
	8	$h_e =$ the length of an edge $e \in \mathbb{E}_h$.	

Chapter 4

Fully Discrete Convex Splitting Scheme

Numerical approximations for modeling microemulsions using the Gompper model has been presented by Hoppe and Linsenmann in [12] also using the C^0 interior penalty method however, the results derived do not establish unconditional unique solvability and no energy stability is presented. Our proposed scheme presented in this chapter addresses both these concerns the latter is shown numerically in Chapter 5.

4.1 Weak Form

Following [13], the dynamics of phase transitions in ternary oil-water-surfactant systems is given by the following conservation law

$$\partial_t \phi - \nabla \cdot (M(\nabla \mu)) = 0 \tag{4.1}$$

where $M \equiv M(\phi) = 1 > 0$ is the mobility and μ is the chemical potential differences between the phases given by $\delta_\phi E$, the variational derivative of the energy functional E with respect to ϕ :

$$\mu := \delta_\phi E = \delta_\phi f_0(\phi) + \delta_\phi \left(\frac{1}{2} \phi^2 |\nabla \phi|^2 \right) + 4\Delta \phi + \Delta^2 \phi. \tag{4.2}$$

We augment (4.1) with the initial value condition

$$\phi(0) = \phi_0 \in H^4(\Omega) \text{ such that } \mathbf{n} \cdot \nabla \phi_0 = 0, \tag{4.3}$$

and the homogeneous Neumann type boundary conditions

$$\mathbf{n} \cdot \nabla \phi = \mathbf{n} \cdot \nabla \Delta \phi = \mathbf{n} \cdot \nabla \mu = 0. \quad (4.4)$$

We note that $\delta_\phi f_0(\phi) = \phi^5 - \phi^3$ and

$$\delta_\phi \left(\frac{1}{2} \phi^2 |\nabla \phi|^2 \right) = \phi |\nabla \phi|^2 - \nabla \cdot (\phi^2 \nabla \phi). \quad (4.5)$$

The system becomes:

$$\partial_t \phi - \nabla \cdot (M \nabla \mu) = 0, \quad (4.6a)$$

$$\phi^5 - \phi^3 + \phi |\nabla \phi|^2 - \nabla \cdot (\phi^2 \nabla \phi) + 4\Delta \phi + \Delta^2 \phi - \mu = 0. \quad (4.6b)$$

The weak formulation of (4.6) relies on the spaces

$$Z := \{z \in H^2(\Omega) \mid \mathbf{n} \cdot \nabla z = 0 \text{ on } \partial\Omega\}, \quad V = H^1(\Omega)$$

and amounts to seeking $(\phi, \mu) \in Z \times V$ satisfying

$$\langle \partial_t \phi, \nu \rangle + (M(\phi) \nabla \mu, \nabla \nu) = 0, \quad \forall \nu \in V \quad (4.7a)$$

$$(\phi^5 - \phi^3 + \phi |\nabla \phi|^2, \psi) + a(\phi, \psi) + ((\phi^2 - 4) \nabla \phi, \nabla \psi) - (\mu, \psi) = 0 \quad \forall \psi \in Z \quad (4.7b)$$

for almost all $0 < t \leq T$ with the compatible initial data (4.3), boundary conditions (4.4) and where $a(u, v) := (\nabla^2 u : \nabla^2 v)$ is the Frobenius inner product of the matrices $\nabla^2 u$ and $\nabla^2 v$. Here and in the sequel, we employ the standard notation for well-known Sobolev spaces and the norms and inner products defined on them. Our numerical scheme is based on a variant of the Eyre's convex splitting scheme in conjunction with the C^0 interior penalty method [3] and backward Euler for the space-time discretization.

4.2 Time Discretization

Let M be a positive integer such that $t_m = t_{m-1} + \tau$ for $1 \leq m \leq M$ where $t_0 = 0$, $t_M = t_F$ with $\tau = \frac{t_F}{M}$ and denote by ϕ^m an approximation of ϕ at time t_m and define the numerical

time derivative as $\delta_\tau \phi := \frac{\phi^{m+1} - \phi^m}{\tau}$. To describe our time splitting scheme, we decompose the energy E (1.2) into $E = E_i + E_e + E_{ie}$ so that (4.6) becomes

$$\delta_\tau \phi^m = \nabla \cdot \nabla \mu^m, \quad (4.8a)$$

$$\mu^m = \delta_\phi E_i(\phi^m) + \delta_\phi E_e(\phi^{m-1}) + \delta_\phi E_{ie}(\phi^{m-1}, \phi^m), \quad (4.8b)$$

where $\delta_\phi E_i(\phi) = \phi^5 + \Delta^2 \phi$ is treated implicitly, $\delta_\phi E_e(\phi) = -\phi^3 + 4\Delta \phi$ is treated explicitly and

$$\delta_\phi E_{ie}(\phi^{m-1}, \phi^m) = \phi^m |\nabla \phi^{m-1}|^2 - \nabla \cdot ((\phi^{m-1})^2 \nabla \phi^m).$$

The weak formulation (4.7) becomes: given $(\phi^{m-1}, \mu^{m-1}) \in Z \times V$, find $(\phi^m, \mu^m) \in Z \times V$ such that

$$(\delta_\tau \phi^m, \nu) + (\nabla \mu^m, \nabla \nu) = 0, \quad (4.9a)$$

$$\begin{aligned} & ((\phi^m)^5 + \phi^m |\nabla \phi^{m-1}|^2 - (\phi^{m-1})^3, \psi) + ((\phi^{m-1})^2 \nabla \phi^m - 4 \nabla \phi^{m-1}, \nabla \psi) \\ & + a(\phi^m, \psi) - (\mu^m, \psi) = 0 \end{aligned} \quad (4.9b)$$

holds for each $(\psi, \nu) \in Z \times V$, $1 \leq m \leq M$ and satisfying the initial condition ϕ^0 (4.3) and μ^0 is constructed using ϕ^0 and (4.6b).

We note the time stepping scheme (4.9) is a modification of the Eyre's convex splitting scheme where the convex energy is treated implicitly and the concave component is treated explicitly.

4.2.1 Fully Discrete C^0 Interior Penalty Method

For presenting the spacial discretization, we let \mathcal{T}_h be a geometrically conforming simplicial triangulation of Ω and recall the following notation:

- $h_K =$ diameter of triangle K ($h = \max_{K \in \mathcal{T}_h} h_K$),
- $v_K =$ restriction of the function v to the triangle K ,
- $|K| =$ area of the triangle K ,

- \mathbb{E}_h = the set of the edges of the triangles in \mathcal{T}_h ,
- e = the edge of a triangle,
- $|e|$ = the length of the edge,
- $Z_h := \{v \in C(\bar{\Omega}) | v_K \in P_2(K) \forall K \in \mathcal{T}_h\}$ the standard finite element space associated with \mathcal{T}_h of degree 2,
- $V_h := \{v \in C(\bar{\Omega}) | v_K \in P_1(K) \forall K \in \mathcal{T}_h\}$ the standard Lagrange finite element spaces associated with \mathcal{T}_h of degree 1.

Accordingly, we seek the continuous approximations $(\phi_h^m, \mu_h^m) \in Z_h \times V_h$ to (4.9) satisfying

$$(\delta_\tau \phi_h^m, \nu) + (\nabla \mu_h^m, \nabla \nu) = 0, \quad \forall \nu \in V_h \quad (4.10a)$$

$$\begin{aligned} & ((\phi_h^m)^5 - \varphi_h^m |\nabla \phi_h^{m-1}|^2 - (\phi_h^{m-1})^3, \psi) + ((\phi_h^{m-1})^2 \nabla \phi_h^m - 4 \nabla \phi_h^{m-1}, \nabla \psi) \\ & + a_h^{IP}(\phi_h^m, \psi) - (\mu_h^m, \psi) = 0 \quad \forall \psi \in Z_h, \end{aligned} \quad (4.10b)$$

with initial data taken to be $\phi_h^0 := P_h \phi_0 = P_h \phi(0)$ where $P_h : Z \rightarrow Z_h$ is a Ritz projection operator such that

$$a_h^{IP}(P_h \phi - \phi, \xi) = 0 \quad \forall \xi \in V_h, \quad (P_h \phi - \phi, 1) = 0, \quad (4.11)$$

Here

$$\begin{aligned} a_h^{IP}(w, v) := & \sum_{K \in \mathcal{T}_h} \int_K (\nabla^2 w : \nabla^2 v) dx + \sum_{e \in \mathbb{E}_h} \int_e \left[\left[\frac{\partial^2 w}{\partial n_e^2} \right] \left[\frac{\partial v}{\partial n_e} \right] \right] dS \\ & + \sum_{e \in \mathbb{E}_h} \int_e \left[\left[\frac{\partial^2 v}{\partial n_e^2} \right] \left[\frac{\partial w}{\partial n_e} \right] \right] dS + \alpha \sum_{e \in \mathbb{E}_h} \frac{1}{|e|} \int_e \left[\left[\frac{\partial w}{\partial n_e} \right] \left[\frac{\partial v}{\partial n_e} \right] \right] dS, \end{aligned} \quad (4.12)$$

with $\alpha \geq 1$ known as a penalty parameter used to weakly enforce the homogeneous Neumann boundary condition. The jumps and averages that appear in (4.12) are defined as follows. For an interior edge e shared by two triangles K_\pm where n_e points from K_- to K_+ , we define on the edge e

$$\left[\left[\frac{\partial v}{\partial n_e} \right] \right] = n_e \cdot (\nabla v_+ - \nabla v_-) \quad \text{and} \quad \left[\left[\frac{\partial^2 v}{\partial n_e^2} \right] \right] = \frac{1}{2} \left(\frac{\partial^2 v_-}{\partial n_e^2} + \frac{\partial^2 v_+}{\partial n_e^2} \right), \quad (4.13)$$

where $\frac{\partial^2 u}{\partial n_e^2} = n_e \cdot (\nabla^2 u) n_e$ and where $v_{\pm} = v|_{K_{\pm}}$. For a boundary edge e which is an edge of the triangle $K \in \mathcal{T}_h$, we take n_e to be the unit normal pointing towards the outside of Ω and define on the edge e ;

$$\left[\left[\frac{\partial v}{\partial n_e} \right] \right] = -n_e \cdot \nabla v_K \quad \text{and} \quad \left[\left[\frac{\partial^2 v}{\partial n_e^2} \right] \right] = n_e \cdot (\nabla^2 v) n_e. \quad (4.14)$$

Remark 4.2.1. Note that the definitions (4.13) and (4.14) are independent of the choice of K_{\pm} , or equivalently, independent of the choice of n_e .

The accuracy of the C^0 -IP method is measured by the following mesh dependent norm

$$\|v_h\|_{2,h}^2 := a(v_h, v_h) + \sum_{e \in \mathbb{E}_h} \frac{\alpha}{|e|} \left\| \left[\left[\frac{\partial v}{\partial n_e} \right] \right] \right\|_{L^2(e)}^2. \quad (4.15)$$

The following lemma guarantees the boundedness of $a_h^{IP}(\cdot, \cdot)$ and is has been shown in [2] and presented in Chapter 3.

Lemma 4.2.1 (Boundedness of $a_h^{IP}(\cdot, \cdot)$). *There exists positive constants C_{cont} and C_{coer} such that for choices of the penalty parameter α large enough we have*

$$a_h^{IP}(w_h, v_h) \leq C_{cont} \|w_h\|_{2,h} \|v_h\|_{2,h} \quad \forall w_h, v_h \in V_h, \quad (4.16)$$

$$C_{coer} \|w_h\|_{2,h}^2 \leq a_h^{IP}(w_h, w_h) \quad \forall w_h \in V_h, \quad (4.17)$$

where the constants C_{cont} and C_{coer} depend only on the shape regularity of \mathcal{T}_h .

4.3 Unconditional Unique Solvability

For proving the unique solvability of the fully discrete scheme (4.10), we need to rely on nonlinear operator analysis techniques similar to [6]. To this end, we first introduce the spaces

$$\begin{aligned} L_0^2(\Omega) &:= \{v \in L^2(\Omega) \mid (v, 1) = 0\}, & \mathring{H}^1(\Omega) &:= H^1(\Omega) \cap L_0^2(\Omega), \\ \mathring{H}_N^{-1}(\Omega) &:= \{v \in H_N^{-1}(\Omega) \mid \langle v, 1 \rangle = 0\}, & \mathring{Z}_h &:= Z_h \cap L_0^2(\Omega), \text{ and } \mathring{V}_h := V_h \cap L_0^2(\Omega). \end{aligned}$$

The operator $\mathbb{T} : \mathring{H}_N^{-1}(\Omega) \rightarrow \mathring{H}^1(\Omega)$ is often referred to as the ‘inverse Laplacian’ and is defined via the following variational problem: given $\zeta \in \mathring{H}^{-1}(\Omega)$, find $\mathbb{T}\zeta \in \mathring{H}^1(\Omega)$ such that

$$(\nabla \mathbb{T}\zeta, \nabla \chi) = \langle \zeta, \chi \rangle \quad \forall \chi \in \mathring{H}^1(\Omega). \quad (4.18)$$

The well posedness of the operator \mathbb{T} is well known, see for example [5], and an induced negative norm may be defined such that $\|v\|_{\mathring{H}_N^{-1}} = (\nabla \mathbb{T}v, \nabla \mathbb{T}v)^{\frac{1}{2}} = \langle v, \mathbb{T}v \rangle^{\frac{1}{2}} = \langle \mathbb{T}v, v \rangle^{\frac{1}{2}}$. We furthermore define a discrete analog of the inverse Laplacian, $\mathbb{T}_h : \mathring{Z}_h \rightarrow \mathring{Z}_h$, via the variational problem: given $\zeta \in \mathring{Z}_h$, find $\mathbb{T}_h\zeta \in \mathring{Z}_h$ such that

$$(\nabla \mathbb{T}_h\zeta_h, \nabla \chi_h) = (\zeta_h, \chi_h) \quad \forall \chi_h \in \mathring{Z}_h. \quad (4.19)$$

Again, the well posedness of the operator \mathbb{T}_h is well known and an induced discrete negative norm on \mathring{W}_h is defined as

$$\|v_h\|_{-1,h} = (\nabla \mathbb{T}_h v_h, \nabla \mathbb{T}_h v_h)^{\frac{1}{2}} = (v_h, \mathbb{T}_h v_h)^{\frac{1}{2}} = (\mathbb{T}_h v_h, v_h)^{\frac{1}{2}}.$$

Remark 4.3.1. *The scheme (4.10) satisfies the discrete conservation property $(\phi_h^m, 1) = (\phi_h^0, 1) = (\phi_0, 1)$ for any $1 \leq m \leq M$. This is easy to see by choosing $\nu_h \equiv 1$ in (4.10a). The quantity $\frac{1}{|\Omega|}(\phi_0, 1)$ is referred to as the average of ϕ_0 over Ω and is denoted by $\bar{\phi}_0$. Due to the discrete conservation property, it follows that $(\phi_h^m, 1) = (\phi_h^0, 1) = |\Omega| \bar{\phi}_0$.*

We prove the unique solvability for any choice of τ and h and for any model parameters by first establishing the existence and uniqueness of the solution for the following intermediate problem (4.20)- (4.10b) and then, proving the equivalence of (4.10a)- (4.10b) and this intermediate problem. For any $1 \leq m \leq M$, given $\varphi_h^{m-1} \in \mathring{Z}_h$ find $(\varphi_h, \mu_{h,\star}) \in \mathring{Z}_h \times \mathring{V}_h$ such that

$$\begin{aligned} a_h^{IP}(\varphi_h^m, \psi_h) + \left((\varphi_h^m + \bar{\phi}_0)^5, \psi_h \right) - \left((\varphi_h^m + \bar{\phi}_0) |\nabla \varphi_h^{m-1}|^2, \psi \right) - \left((\varphi_h^{m-1} + \bar{\phi}_0) |\nabla \varphi_h^m|^2, \psi \right) \\ - (\mu_{h,\star}^m, \psi_h) = \left((\varphi_h^{m-1} + \bar{\phi}_0)^3, \psi_h \right) - 4 (\nabla \varphi_h^{m-1}, \nabla \psi_h) \end{aligned} \quad (4.20)$$

for all $\psi_h \in \mathring{Z}_h$, where $\mu_{h,\star}^m \in \mathring{V}_h$ is the unique solution to

$$(\nabla \mu_{h,\star}^m, \nabla \nu_h) = - \left(\frac{\varphi_h^m - \varphi_h^{m-1}}{\tau}, \nu_h \right) \quad \forall \nu_h \in \mathring{V}_h. \quad (4.21)$$

The existence and uniqueness of the intermediate formulation (4.20)- (4.21) is proved through the properties of the following functional G_h . Let $\varphi_h^{m-1} \in \mathring{Z}_h$ be given. For all $\varphi_h \in \mathring{Z}_h$, define the nonlinear functional

$$G_h(\varphi_h) := \frac{\tau}{2} \left\| \frac{\varphi_h - \varphi_h^{m-1}}{\tau} \right\|_{-1,h}^2 + \frac{1}{2} a_h^{IP}(\varphi_h, \varphi_h) + \frac{1}{6} \|\varphi_h + \bar{\phi}_0\|_{L^6(\Omega)}^6 + \frac{1}{2} \|\varphi_h^{m-1} \nabla \varphi_h\|_{L^2(\Omega)}^2 + \frac{1}{2} \|(\varphi_h + \bar{\phi}_0) \nabla \varphi_h^{m-1}\|_{L^2(\Omega)}^2 - \left((\varphi_h^{m-1})^3, \varphi_h \right) - 4 (\nabla \varphi_h^{m-1}, \nabla \varphi_h). \quad (4.22)$$

The following lemma proves the properties of G_h .

Lemma 4.3.1. *The functional G_h given by (4.22) is strictly convex and coercive on the linear subspace \mathring{Z}_h . Consequently, G_h has a unique minimizer, call it $\varphi_h^m \in \mathring{Z}_h$. Moreover, $\varphi_h^m \in \mathring{Z}_h$ is the unique minimizer of G_h if and only if it is the unique solution to (4.20)- (4.21).*

Proof. We begin by showing G_h is strictly convex. To do so, we consider the second derivative of $G_h(\varphi_h + s\psi)$ with respect to s and set $s = 0$. Hence,

$$G_h(\varphi_h + s\psi) = \frac{\tau}{2} \left\| \frac{\varphi_h + s\psi - \varphi_h^{m-1}}{\tau} \right\|_{-1,h}^2 + \frac{1}{2} a_h^{IP}(\varphi_h + s\psi, \varphi_h + s\psi) + \frac{1}{6} \|\varphi_h + s\psi + \bar{\phi}_0\|_{L^6(\Omega)}^6 + \frac{1}{2} \|(\varphi_h + \bar{\phi}_0 + s\psi) \nabla \varphi_h^{m-1}\|_{L^2(\Omega)}^2 + \frac{1}{2} \|\varphi_h^{m-1} \nabla(\varphi_h + s\psi)\|_{L^2(\Omega)}^2 - \left((\varphi_h^{m-1})^3, \varphi_h + s\psi \right) - 4 (\nabla \varphi_h^{m-1}, \nabla(\varphi_h + s\psi)).$$

Taking the derivative with respect to s , we have

$$G'_h(\varphi_h + s\psi) = \frac{1}{\tau} (\varphi_h + s\psi - \varphi_h^{m-1}, \psi)_{-1,h} + a_h^{IP}(\varphi_h + s\psi, \psi) + \left((\varphi_h + s\psi + \bar{\phi}_0)^5, \psi \right) + \left((\varphi_h + \bar{\phi}_0) \nabla \varphi_h^{m-1}, \psi \nabla \varphi_h^{m-1} \right) + (s\psi \nabla \varphi_h^{m-1}, \psi \nabla \varphi_h^{m-1}) + (\varphi_h^{m-1} \nabla \varphi_h, \varphi_h^{m-1} \nabla \psi) + (s\varphi_h^{m-1} \nabla \psi, \varphi_h^{m-1} \nabla \psi) + \left((\varphi_h^{m-1})^2 \nabla \varphi_h, \nabla \psi \right) - 4 (\nabla \varphi_h^{m-1}, \nabla \psi), \quad (4.23)$$

where $(\zeta, \xi)_{-1,h} := (\zeta, \mathbb{T}_h \xi)$. Taking the second derivative with respect to s , we have

$$G''_h(\varphi_h + s\psi) = \frac{1}{\tau} \|\psi\|_{-1,h}^2 + a_h^{IP}(\psi, \psi) + 5 \left((\varphi_h + s\psi + \bar{\phi}_0)^4, \psi^2 \right) + \|\psi \nabla \varphi_h^{m-1}\|_{L^2(\Omega)}^2 + \|\varphi_h^{m-1} \nabla \psi\|_{L^2(\Omega)}^2.$$

Setting $s = 0$ and using the coercivity of $a_h^{IP}(\cdot, \cdot)$, we have

$$\begin{aligned} G_h''(\varphi_h) &= \frac{1}{\tau} \|\psi\|_{-1,h}^2 + a_h^{IP}(\psi, \psi) + 5 \left((\varphi_h + \bar{\phi}_0)^4, \psi^2 \right) \\ &\quad + \|\psi \nabla \varphi_h^{m-1}\|_{L^2(\Omega)}^2 + \|\varphi_h^{m-1} \nabla \psi\|_{L^2(\Omega)}^2 > 0 \end{aligned}$$

for all $\varphi_h \in \mathring{Z}_h$.

To show G_h is coercive, we need to show that there exists constants $\gamma > 0, \beta \geq 0$ such that $G_h(\varphi_h) \geq \gamma \|\varphi_h\|_{2,h} - \beta$ for all $\varphi_h \in V_h$. Using the Cauchy Schwartz inequality, Young's inequality, and Poincarè's inequality,

$$G_h(\varphi_h) \geq C_0 \|\varphi_h\|_{2,h}^2 - C_1 \|\nabla \varphi_h^{m-1}\|_{L^2(\Omega)}^2 - C_2 \|\varphi_h\|_{2,h}^2,$$

where C_0 depends on the coercivity of the $a_h^{IP}(\cdot, \cdot)$ inner product, C_1 depends on the Poincarè constant, and C_2 is chosen to be less than C_0 . Therefore,

$$G_h(\varphi_h) \geq \gamma \|\varphi_h\|_{2,h}^2 - \beta,$$

where $\gamma = C_0 - C_2$ and $\beta = C_1 \|\nabla \varphi_h^{m-1}\|_{L^2(\Omega)}^2$ do not depend on φ_h . Hence, G_h has a unique minimizer, $\varphi_h^m \in \mathring{Z}_h$ which solves

$$\begin{aligned} G_h'(\varphi_h^m) &= \frac{1}{\tau} (\varphi_h^m - \varphi_h^{m-1}, \psi)_{-1,h} + a_h^{IP}(\varphi_h^m, \psi) + \left((\varphi_h^m + \bar{\phi}_0)^5, \psi \right) + \left((\varphi_h^{m-1})^3, \psi \right) \\ &\quad - 4 (\nabla \varphi_h^{m-1}, \nabla \psi) = 0, \end{aligned}$$

for all $\psi \in \mathring{Z}_h$ where we have set $s = 0$ in [\(4.23\)](#). Therefore, $\varphi_h^m \in \mathring{Z}_h$ is the unique minimizer of G_h if and only if it is the unique solution to

$$\begin{aligned} (\mu_{h,\star}^m, \psi_h) - a_h^{IP}(\varphi_h^m, \psi_h) - \left((\varphi_h^m + \bar{\phi}_0)^5, \psi_h \right) + \left((\varphi_h^{m-1} + \bar{\phi}_0)^3, \psi_h \right) + 4 (\nabla \varphi_h^{m-1}, \nabla \psi_h) \\ - \left((\varphi_h^m + \bar{\phi}_0) |\nabla \varphi_h^{m-1}|^2, \psi \right) - \left((\varphi_h^{m-1} + \bar{\phi}_0) |\nabla \varphi_h^m|^2, \psi \right) = 0 \end{aligned}$$

for all $\psi_h \in \mathring{Z}_h$, where $\mu_{h,\star}^m \in \mathring{V}_h$ is the unique solution to

$$(\nabla \mu_{h,\star}^m, \nabla \nu_h) = - \left(\frac{\varphi_h^m - \varphi_h^{m-1}}{\tau}, \nu_h \right) \quad \forall \nu_h \in \mathring{V}_h.$$

□

Theorem:

The scheme (4.20) – (4.21), or, equivalently, the scheme (4.10a) – (4.10b), is uniquely solvable for any mesh parameters τ and h .

Proof. Suppose $(\varphi_h^{m-1}, 1) = 0$. It is clear that a necessary condition for solvability of (4.20) – (4.21) is that

$$(\varphi_h^m, 1) = (\varphi_h^{m-1}, 1) = 0, \quad (4.24)$$

as can be found by taking $\nu_h \equiv 1$ in (4.21). Now, let $(\varphi_h^m, \mu_{h,\star}^m) \in \mathring{Z}_h \times \mathring{V}_h$ be a solution of (4.20) – (4.21). Set

$$\overline{\mu}_h^m := \frac{1}{|\Omega|} \left((\varphi_h^m + \overline{\phi}_0)^5 - (\varphi_h^{m-1} + \overline{\phi}_0)^3, 1 \right) \quad (4.25)$$

and define $\mu_h^m := \mu_{h,\star}^m + \overline{\mu}_h^m$. There is a one-to-one correspondence of the respective solution sets: $\varphi_h^m, \mu_{h,\star}^m \in \mathring{Z}_h \times \mathring{V}_h$ is a solution to (4.20) – (4.21) if and only if $\phi_h^m, \mu_h^m \in Z_h \times V_h$ is a solution to (4.10a) – (4.10b), where

$$\phi_h^m = \varphi_h^m + \overline{\phi}_0, \quad \mu_h^m = \mu_{h,\star}^m + \overline{\mu}_h^m. \quad (4.26)$$

But (4.20) – (4.21) admits a unique solution, which proves that (4.10a) – (4.10b) is uniquely solvable. \square

Chapter 5

Numerical Results

All numerical results are obtained using the FEniCS project [\[1\]](#). Thanks to The Texas Advanced Computing Center (TACC) at The University of Texas at Austin for providing HPC, visualization, database, or grid resources that have contributed to the research results reported within this thesis.

In this chapter, we show that our method converges with first order accuracy with regard to both time and space. We furthermore show that the discrete energy:

$$E(\phi) := \frac{1}{6} \|\phi\|_{L^6(\Omega)}^6 - \frac{1}{4} \|\phi\|_{L^4(\Omega)}^4 + \frac{1}{2} \|\phi \nabla \phi\|_{L^2(\Omega)}^2 - 2 \|\nabla \phi\|_{L^2(\Omega)}^2 + \frac{1}{2} a_h^{IP}(\phi, \phi) + \frac{|\Omega|}{12}.$$

dissipates over time. To demonstrate this, we consider two tests.

5.0.1 Accuracy Test

The first tests the accuracy of the method. We set the initial conditions to be:

$$\phi(x, y) = 0.3 \cos(3x) + 0.5 \cos(y)$$

and solve on the domain $\Omega = [0, 2\pi]^2$ to a final stopping time of $T = 0.1$. We solve using the mesh sizes shown in the table below and scale the time step size with the mesh size via $\tau = 0.05h$. We set the mobility as $M(\phi) \equiv 1$, and the penalty parameter $\alpha = 20$. We point out that Neumann boundary conditions are implemented and the finite element space utilizes P_2 Lagrange finite elements. To show first order convergence in the energy norm, we let the solution from a mesh size of $h = \frac{2\pi}{2}$ with τ with $\tau = 0.05h$ and $T = 0.1$ as the ‘exact’ solution, ϕ_{exact} . Then we define $\delta_\phi := \phi_h - \phi_{exact}$, where ϕ_h indicates the

solution on the mesh size h with $\tau = 0.05h$ and $T = 0.1$. Table 5.1 shows the errors and rates of convergence given the parameters noted in the text above. We solve the resultant nonlinear system using Newton’s solver.

The number of Newton’s iterations needed for convergence stays constant at 3. Time

Table 5.1: Errors and convergence rates of the C^0 -IP method. Parameters and initial conditions are given in the text.

h	$\ \delta\phi\ _{L^2}$	$\ \delta\phi\ _{2,h}$	rate
$\frac{2\pi}{2}$	2.041987039187612	52.2412	–
$\frac{2\pi}{4}$	0.5610049780129817	4.0433	–
$\frac{2\pi}{8}$	0.0761185133187028	0.9087	1.7972358771640413
$\frac{2\pi}{16}$	0.054101647325269085	0.14239	1.054682778650358
$\frac{2\pi}{32}$	0.02834778857415166	0.03203	1.2631240026538169
$\frac{2\pi}{64}$	0.014612189335501178	0.00780	1.0541769089838793

evolution of the free energy functional is seen in Examples 5.0.1 and 5.0.2. The energy curves show monotone decays for both.

5.0.2 Formation of oil-in-water and water-in-oil droplets

We present a visualization of the microemulsification process obtained by the numerical solution of the sixth order Cahn-Hilliard equation.

The pure water phase $\phi = 1$ is depicted and $\phi = -1$ corresponds to pure oil phase and microemulsification at $c = 0$. We set the initial conditions to be the randomly perturbed concentration fields:

$$\phi(x, y) = \bar{\phi}_0 + \gamma \text{rand}(x, y),$$

where $\text{rand}(x, y)$ denotes a random number between -1 and 1 and $\bar{\phi}_0$ denotes a homogeneous concentration and $\gamma = 0.001$.

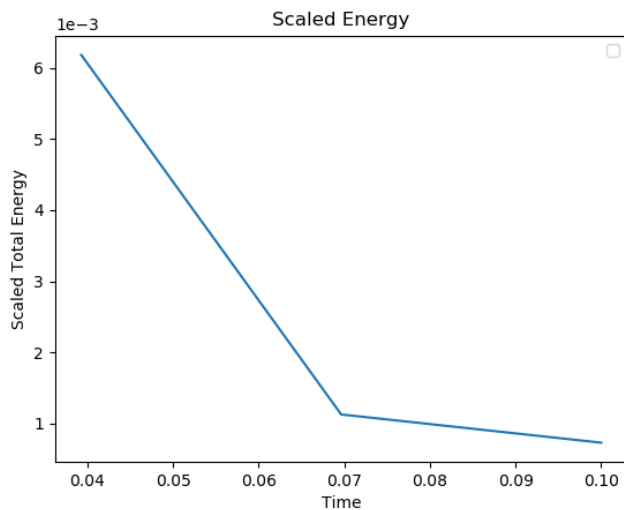


Figure 5.1:

The time evolution of the scaled total energy $\frac{(F - \frac{|\Omega|}{12})}{|\Omega|}$. The mesh size is $h = \frac{2\pi}{256}$ and $\tau = 0.05h$. All other parameters are defined in the text. cases.

- In a homogeneous mixture, we introduce a randomized concentration field and place a weight of γ which controls the level of randomized input.
- We set the mesh size at $\frac{2\pi}{128}$ and extend the time to $T = 1$.

Initially, the two fluids are well mixed, and they sooner start to decompose due to surface tensions. We present results for:

$$\bar{\phi}_0 = -0.5, \quad \gamma = 0.001, 0.1.$$

What is crucial to observe is the time step on which the dynamics appears. Our final time here is $T = 0.1$ with 407 snapshots of concentration. While the pictures evolve very quickly within the first 100 time steps.

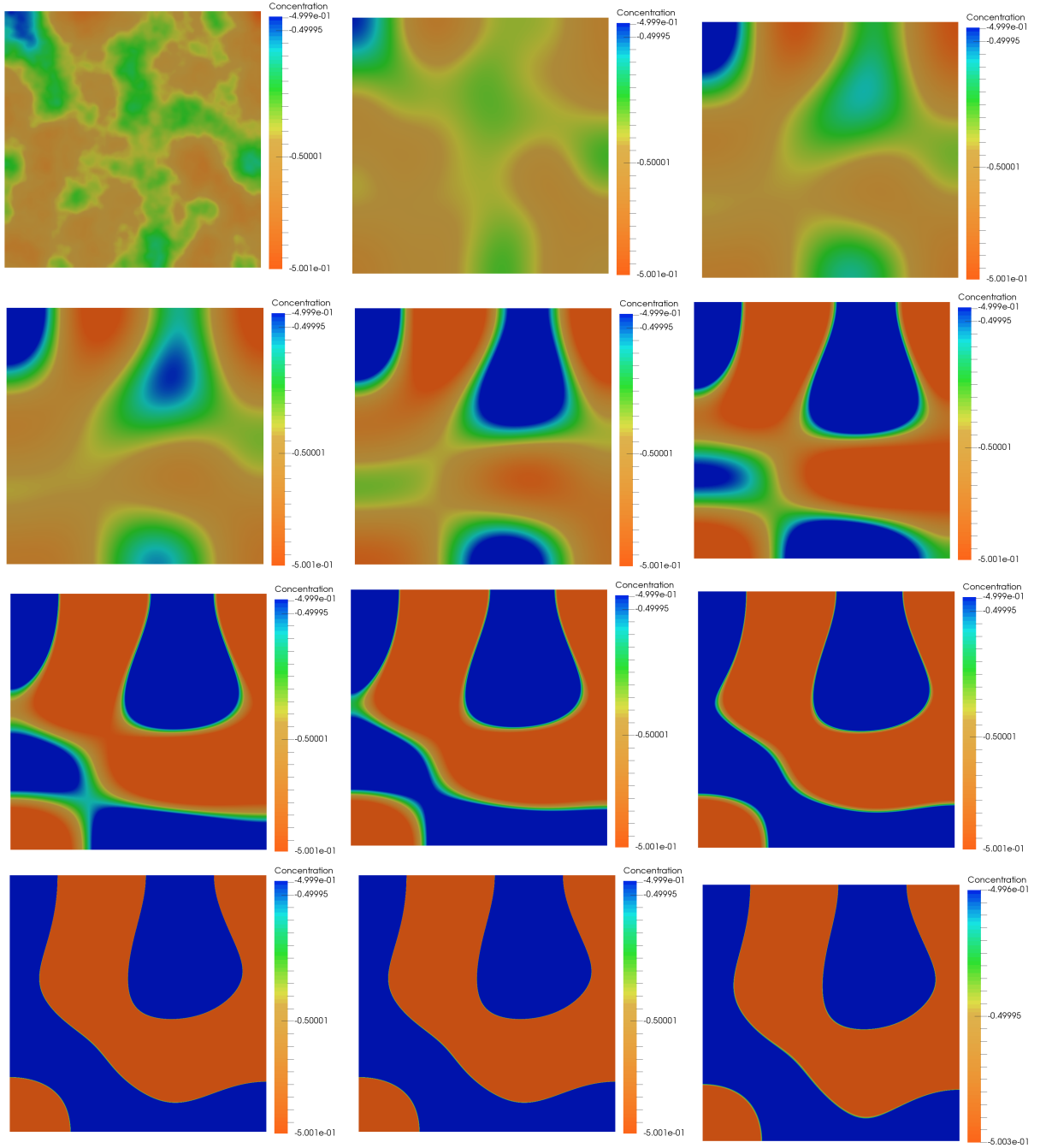


Figure 5.2: $\bar{\phi}_0 = -0.5$, $\gamma = 0.001$; Evolution over time top left snapshot of initial random configuration. The bifurcation times and their snapshots are presented. The snapshots at timesteps 3,62,78,126,180,210,229,255 and 290, 350 and final time at time step 407.

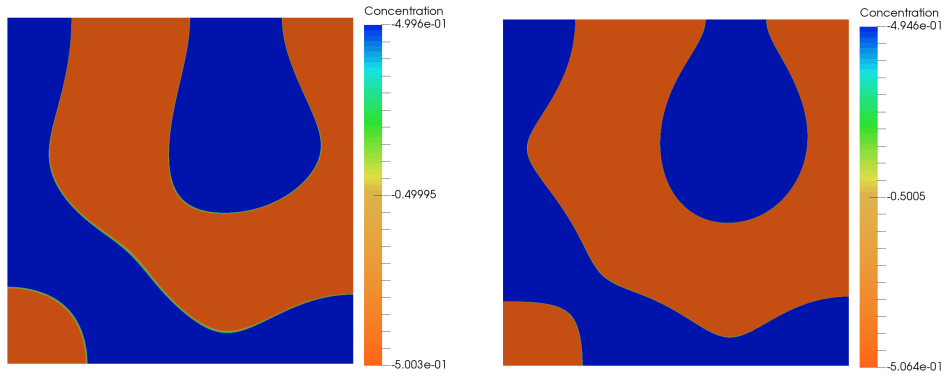


Figure 5.3: Left: $\bar{\phi}_0 = -0.5$, $\gamma = 0.1$; Right: $\bar{\phi}_0 = -0.5$, $\gamma = 0.5$ at final time $T = 4$.

We remark that in this figure (5.3), irrespective of γ , if we extend the final time to $T = 4$, we observe the dominance of the energy;

$\left(\frac{1}{6} \int_{\Omega} (\phi + 1)^2 (\phi^2 + 0.5) (\phi - 1)^2 dx \right)$ corresponding to separation of phases.

Chapter 6

Conclusion

6.1 Significance of the Result

6.1.1 Significance of Mathematical Modeling of Microemulsions

1. Modeling Microemulsions is of immense relevance particularly in pharmaceutical industries where the formation and disappearance as well as the stability of the microemulsion is of great significance. This is effective in predicting the outcome of experiments numerically before actually conducting the physical experiments.
2. Microemulsions are generally wonderful. They have unique distinguishing features like enhanced bioavailability due to their ability to solubilize lipophilic drugs [15].
3. They have and can carry water-soluble drugs into aqueous phase, and hence demonstrate the ability to carry both lipophilic as well as hydrophilic drugs [15].
4. They have extensive protection from hydrolysis and oxidation.
5. They demonstrate greater longevity.

Clearly, modeling of microemulsions is absolute necessary and significant and has thus caused great breakthroughs in science particularly in pharmaceutical industries.

6.1.2 Applications of Microemulsions in Drug Delivery

Microemulsion formulations are normally beneficial over the conventional oral formulations for oral drug administration/delivery. They offer increased absorption, enhanced clinical

potency, and less drug toxicity. Thus microemulsions have been scientifically reported to be more ideal delivery carriers of drugs such as hormones, steroids, antibiotics, and diuretics [4]. The oral route is the major route for drug delivery in many diseases. The major problem that we face in the delivery of oil-soluble drugs in the oral route is the poor aqueous solubility. One way to sort out this problem is to deliver the drug in the microemulsion form.

Modeling an effective oral delivery system has always been problematic for scientists and researchers, because of poor solubility and instability of the drugs in the GI fluid. Microemulsions have the unique ability to circumvent these problems [10]. Microemulsions encapsulate the drugs with varying solubility because of the presence of polar, nonpolar, and interfacial domains in them [15]. Microemulsions protect the incorporated drugs from oxidative and enzymatic degradation. The absorption efficiency of levofloxacin hemihydrate, a synthetic quinolone antibiotic, was found to be enhanced by the use of a water-in-oil microemulsion system [10] thus proving generally useful in drug delivery.

6.2 Future Work

Our next phase is twofold: to improve our time-stepping scheme and replace it with an adaptive scheme. To use real data provided by the laboratory experiments and test the effectiveness of our numerical method/ simulation against physical experiments.

Bibliography

- [1] M. Alnæs, J. Blechta, J. Hake, A. Johansson, B. Kehlet, A. Logg, C. Richardson, J. Ring, M. E. Rognes, and G. N. Wells. The FEniCS project version 1.5. *Archive of Numerical Software*, 3(100), 2015.
- [2] S. C. Brenner. C^0 interior penalty methods. In *Frontiers in Numerical Analysis-Durham 2010*, pages 79–147. Springer, 2011.
- [3] S. C. Brenner and L.-Y. Sung. C^0 interior penalty methods for fourth order elliptic boundary value problems on polygonal domains. *J Sci. Comput.*, 22(1-3):83–118, 2005.
- [4] William N Charman. Lipids, lipophilic drugs, and oral drug delivery—some emerging concepts. *Journal of pharmaceutical sciences*, 89(8):967–978, 2000.
- [5] A. E. Diegel, X. H. Feng, and S. M. Wise. Analysis of a mixed finite element method for a Cahn–Hilliard–Darcy–Stokes system. *SIAM J. Numer. Anal.*, 53(1):127–152, 2015.
- [6] A. E. Diegel and N. Sharma. A C^0 interior penalty method for the phase field crystal equation. preprint.
- [7] DJ EYRE. Unconditionally gradient stable time marching the cahn-hilliard equation. *computational and mathematical models of microstructural evolution*, 53:1686–1712, 1998.
- [8] G Gompper and M Schick. Correlation between structural and interfacial properties of amphiphilic systems. *Physical review letters*, 65(9):1116, 1990.
- [9] G Gompper and S Zschocke. Elastic properties of interfaces in a ginzburg-landau theory of swollen micelles, droplet crystals and lamellar phases. *EPL (Europhysics Letters)*, 16(8):731, 1991.

- [10] Gagan Goyal, Tarun Garg, Basant Malik, Gaurav Chauhan, Goutam Rath, and Amit K Goyal. Development and characterization of niosomal gel for topical delivery of benzoyl peroxide. *Drug delivery*, 22(8):1027–1042, 2015.
- [11] Jean-Baptiste Hiriart-Urruty and Claude Lemaréchal. Convex analysis and minimization algorithms i, volume 305 of comprehensive study in mathematics, 1993.
- [12] R. H. W. Hoppe and C. Linsenmann. C^0 -interior penalty discontinuous Galerkin approximation of a sixth-order Cahn-Hilliard equation. *Contrib. PDEs Appl.*, 47:297, 2018.
- [13] I. Pawłow and W. Zajaczkowski. A sixth order Cahn–Hilliard type equation arising in oil-water-surfactant mixtures. *Communications on Pure and Applied Analysis*, 10:1823–1847, 11 2011.
- [14] Leon Prince. *Microemulsions theory and practice*. Elsevier, 2012.
- [15] Aman Kumar Sharma, Tarun Garg, Amit K. Goyal, and Goutam Rath. Role of microemulsions in advanced drug delivery. *Artificial Cells, Nanomedicine, and Biotechnology*, 44(4):1177–1185, 2016. PMID: 25711493.
- [16] M Teubner and R Strey. Origin of the scattering peak in microemulsions. *The Journal of Chemical Physics*, 87(5):3195–3200, 1987.
- [17] CG Vonk, John F Billman, and Eric W Kaler. Small angle scattering of bicontinuous structures in microemulsions. *The Journal of chemical physics*, 88(6):3970–3975, 1988.

Appendices

Appendix A

Differential Operators

1. Unit vectors:

$$\mathbf{e}_1 = (1, 0)^T, \quad \mathbf{e}_2 = (0, 1)^T$$

2. $\mathbf{x} = (x_1, x_2) = x_1\mathbf{e}_1 + x_2\mathbf{e}_2$.

3. Gradient:

$$\nabla p = \frac{\partial p}{\partial x_1}\mathbf{e}_1 + \frac{\partial p}{\partial x_2}\mathbf{e}_2$$

4. Divergence:

$$\nabla \cdot \mathbf{v} = \frac{\partial v_1}{\partial x_1} + \frac{\partial v_2}{\partial x_2}$$

5. Laplacian:

$$\Delta p = \nabla \cdot \nabla p = \frac{\partial^2 p}{\partial x_1^2} + \frac{\partial^2 p}{\partial x_2^2}$$

6. Biharmonic/BiLaplacian:

$$\Delta^2 p = \Delta(\Delta p) = \nabla^4 p = \frac{\partial^4 p}{\partial x_1^4} + 2\frac{\partial^4 p}{\partial x_1^2 \partial x_2^2} + \frac{\partial^4 p}{\partial x_2^4}$$

Appendix B

Theorem: The Gateaux derivative $\delta_\phi E$ of the following energy

$$E(\phi) = \int_{\Omega} \left[\frac{1}{\epsilon} f(\phi) + \frac{\epsilon}{2} |\nabla \phi|^2 \right] dx, \quad f(\phi) = \frac{1}{4} (\phi^2 - 1)^2, \quad \epsilon > 0. \quad (\text{B.1})$$

is

$$\delta_\phi E = \frac{\phi^3 - \phi}{\epsilon} - \epsilon \Delta \phi$$

Proof. Thus we compute $\lim_{\lambda \rightarrow 0^+} \frac{E(\phi + \lambda \Phi) - E(\phi)}{\lambda}$.

$$E(\phi) = \int_{\Omega} \left[\frac{1}{\epsilon} f(\phi) + \frac{\epsilon}{2} |\nabla \phi|^2 \right] dx = \frac{1}{\epsilon} \int_{\Omega} f(\phi) dx + \frac{\epsilon}{2} \int_{\Omega} |\nabla \phi|^2 dx \quad (\text{B.2})$$

$$E(\phi + \lambda \Phi) = \int_{\Omega} \left[\frac{1}{\epsilon} f(\phi + \lambda \Phi) + \frac{\epsilon}{2} |\nabla(\phi + \lambda \Phi)|^2 \right] dx = \frac{1}{\epsilon} \int_{\Omega} f(\phi + \lambda \Phi) dx + \frac{\epsilon}{2} \int_{\Omega} |\nabla \phi + \lambda \nabla \Phi|^2 dx. \quad (\text{B.3})$$

substituting; $|\nabla(\phi + \lambda \nabla \Phi)|^2 = |\nabla \phi|^2 + \lambda(\nabla \phi)^T \nabla \Phi + \lambda(\nabla \Phi)^T \nabla \phi + \lambda^2 |\nabla \Phi|^2$ in [\(B.3\)](#) gives:

$$E(\phi + \lambda \Phi) = \frac{1}{\epsilon} \int_{\Omega} f(\phi + \lambda \Phi) dx + \frac{\epsilon}{2} \int_{\Omega} |\nabla \phi|^2 + \lambda(\nabla \phi)^T \nabla \Phi + \lambda(\nabla \Phi)^T \nabla \phi + \lambda^2 |\nabla \Phi|^2 dx. \quad (\text{B.4})$$

Then,

$$E(\phi + \lambda \Phi) - E(\phi) = \frac{1}{\epsilon} \int_{\Omega} f(\phi + \lambda \Phi) - f(\phi) dx + \frac{\epsilon}{2} \int_{\Omega} \lambda(\nabla \phi)^T \nabla \Phi + \lambda(\nabla \Phi)^T \nabla \phi + \lambda^2 |\nabla \Phi|^2 dx.$$

Now, from the definition of f , we get the terms:

$$f(\phi + \lambda \Phi) - f(\phi) = \frac{1}{4} \left[4\lambda \phi^3 \Phi + 6\lambda^2 \phi^2 \Phi^2 + 4\lambda^3 \phi \Phi^3 + \lambda^4 \Phi^4 - 4\lambda \phi \Phi - 2\lambda^2 \Phi^2 \right]$$

Observe that

$$\frac{E(\phi + \lambda\Phi) - E(\phi)}{\lambda} = \frac{\frac{\lambda}{4\epsilon} \int_{\Omega} \left[4\phi^3\Phi + 6\lambda\phi^2\Phi^2 + 4\lambda^2\phi\Phi^3 + \lambda^3\Phi^4 - 4\phi\Phi - 2\lambda\Phi^2 \right] dx + \frac{\lambda\epsilon}{2} \int_{\Omega} \left[2(\nabla\phi)^T \nabla\Phi + \lambda|\nabla\Phi|^2 \right] dx}{\lambda}$$

letting $\lambda \rightarrow 0^+$

$$\begin{aligned} \lim_{\lambda \rightarrow 0^+} \frac{E(\phi + \lambda\Phi) - E(\phi)}{\lambda} &= \frac{1}{\epsilon} \int_{\Omega} \left(\phi^3\Phi - \phi\Phi \right) dx + \frac{\epsilon}{2} \int_{\Omega} 2(\nabla\phi)^T \nabla\Phi dx \\ &= \frac{1}{\epsilon} \int_{\Omega} \left(\phi^3\Phi - \phi\Phi \right) dx + \epsilon \int_{\Omega} (\nabla\phi)^T \nabla\Phi dx \\ &= \frac{1}{\epsilon} \int_{\Omega} \left(\phi^3\Phi - \phi\Phi \right) dx - \epsilon \int_{\Omega} \nabla \cdot \nabla\phi\Phi + \int_{\Gamma} \frac{\partial\phi}{\partial n} \Phi ds \\ &= \frac{1}{\epsilon} \int_{\Omega} \left(\phi^3\Phi - \phi\Phi \right) dx - \epsilon \int_{\Omega} \Delta\phi\Phi dx \\ &= \int_{\Omega} \left(\frac{\phi^3 - \phi}{\epsilon} - \epsilon\Delta\phi \right) \Phi dx = 0 \quad \forall v \\ &= \frac{\phi^3 - \phi}{\epsilon} - \epsilon\Delta\phi = 0 \end{aligned}$$

where we have used integration by parts and vanishing boundary conditions.

Thus denote $\mu = \epsilon^{-1}(\phi^3 - \phi) - \epsilon\Delta\phi$ which is the chemical potential $\delta_{\phi}E$ denoting the variational derivative of E with respect to ϕ . \square

Appendix C

Theorem: The Gateaux derivative $\delta_\phi E$ of the following energy

$$E(\phi) = F_0(\phi) + G_0(\phi) \quad (\text{C.1})$$

where $\kappa_2 > 0$,

$$G_0(\phi) = \int_{\Omega} \left\{ \frac{a_0 + a_2 \phi^2}{2} |\nabla \phi|^2 + \frac{\kappa_2}{2} (\Delta \phi)^2 \right\} dx$$

and

$$F_0(\phi) = \frac{\beta}{2} \int_{\Omega} (\phi - \phi_o)^2 (\phi^2 + h_0) (\phi - \phi_w)^2 dx \quad (\text{C.2})$$

with $\beta > 0$ is surface energy density and the parameter h_0 measures the deviation from the oil-water-microemulsion coexistence. is

$$\delta_\phi E = \frac{\beta}{2} (6\phi^5 + 4(h_0 - 2)\phi^3 + 2(1 - 2h_0)\phi) - \nabla \cdot (\kappa_1(\phi)\nabla\phi) + \frac{1}{2}\kappa_1'(\phi)|\nabla\phi|^2 + \kappa_2\Delta^2\phi$$

Proof. We express Gateaux Derivative of E w.r.t ϕ as and prove the result for each term on the right hand side.

$$\frac{\delta E(\phi)}{\delta \phi} = \frac{\delta F_0(\phi)}{\delta \phi} + \frac{\delta G_0(\phi)}{\delta \phi}$$

- For $\frac{\delta F_0(\phi)}{\delta \phi}$;

$$\begin{aligned} F_0(\phi + \alpha\Phi) &= \frac{\beta}{2} \int_{\Omega} (\phi + \alpha\Phi + 1)^2 ((\phi + \alpha\Phi)^2 + h_0) (\phi + \alpha\Phi - 1)^2 dx \\ F_0(\phi + \alpha\Phi) - F_0(\phi) &= \frac{\beta}{2} \int_{\Omega} \{ (\phi + \alpha\Phi + 1)^2 ((\phi + \alpha\Phi)^2 + h_0) (\phi + \alpha\Phi - 1)^2 \} \\ &\quad - \{ (\phi + 1)^2 (\phi^2 + h_0) (\phi - 1)^2 \} dx \\ \lim_{\alpha \rightarrow 0} \frac{F_0(\phi + \alpha\Phi) - F_0(\phi)}{\alpha} &= \frac{\beta}{2} \int_{\Omega} \{ 6\phi^5 - 8\phi^3 + 2\phi + 4\phi^3 h_0 - 4\phi h_0 \} \Phi dx \end{aligned}$$

Thus;

$$\frac{\delta F_0(\phi)}{\delta \phi} = \frac{\beta}{2} \{6\phi^5 + 4(h_0 - 2)\phi^3 + 2(1 - 2h_0)\phi\} \quad (\text{C.3})$$

- For $\frac{\delta G_0(\phi)}{\delta \phi}$;

$$\begin{aligned} G_0(\phi + \alpha\Phi) &= \int_{\Omega} \left\{ \frac{\kappa_1(\phi + \alpha\Phi)}{2} |\nabla\phi + \alpha\nabla\Phi|^2 + \frac{\kappa_2}{2} (\Delta\phi + \alpha\Delta\Phi)^2 \right\} dx \\ G_0(\phi + \alpha\Phi) - G_0(\phi) &= \frac{1}{2} \int_{\Omega} \left\{ \kappa_1(\phi + \alpha\Phi) |\nabla\phi + \alpha\nabla\Phi|^2 - \kappa_1(\phi) |\nabla\phi|^2 \right\} \\ &\quad + \left\{ \kappa_2\Delta\phi + \alpha\Delta\Phi \right\}^2 - \kappa_2(\Delta\phi)^2 \Big\} dx \end{aligned}$$

Now;

$$\begin{aligned} \lim_{\alpha \rightarrow 0} \int_{\Omega} \frac{G_0(\phi + \alpha\Phi) - G_0(\phi)}{\alpha} dx &= \int_{\Omega} \kappa_1(\phi) \nabla\phi \cdot \nabla\Phi dx + \frac{1}{2} \int_{\Omega} \kappa_1'(\phi) |\nabla\phi|^2 \Phi dx \\ &\quad + \int_{\Omega} \kappa_2 \Delta\phi \Delta\Phi dx. \end{aligned} \quad (\text{C.4})$$

Each of the terms on the right hand side of [\(C.4\)](#) can be expressed below thanks to integration by parts with the following formulas;

$$\int_{\Omega} \kappa_1(\phi) \nabla\phi \cdot \nabla\Phi dx = - \int_{\Omega} \nabla \cdot (\kappa_1(\phi) \nabla\phi) \Phi dx + \int_{\partial\Omega} \mathbf{n} \cdot (\kappa_1(\phi) \nabla\phi) \Phi ds \quad (\text{C.5})$$

$$\int_{\Omega} \Delta\phi \Delta\Phi dx = \int_{\Omega} \frac{\partial\Delta\phi}{\partial\mathbf{n}} \Phi ds - \int_{\partial\Omega} \frac{\partial^2\phi}{\partial\mathbf{n}^2} \frac{\partial\Phi}{\partial\mathbf{n}} ds + \int_{\Omega} (\Delta^2\phi) \Phi dx. \quad (\text{C.6})$$

Using the fact that $\phi = \partial_{\mathbf{n}}\phi = 0$ and substituting equations [C.5](#) and [C.6](#) into [C.4](#) we have;

$$\lim_{\alpha \rightarrow 0} \int_{\Omega} \frac{G_0(\phi + \alpha\Phi) - G_0(\phi)}{\alpha} dx = \int_{\Omega} \left\{ -\nabla \cdot (\kappa_1(\phi) \nabla\phi) \Phi + \kappa_1'(\phi) |\nabla\phi|^2 \Phi + \kappa_2 \Delta^2\phi \Phi \right\} dx.$$

Thus;

$$\frac{\delta G_0(\phi)}{\delta(\phi)} = -\nabla \cdot (\kappa_1(\phi) \nabla\phi) + \frac{1}{2} \kappa_1'(\phi) |\nabla\phi|^2 + \kappa_2 \Delta^2\phi \quad (\text{C.7})$$

The Gateaux Derivative of E w.r.t ϕ becomes;

$$\frac{\delta E(\phi)}{\delta \phi} = \frac{\beta}{2} (6\phi^5 + 4(h_0 - 2)\phi^3 + 2(1 - 2h_0)\phi) - \nabla \cdot (\kappa_1(\phi)\nabla\phi) + \frac{1}{2}\kappa_1'(\phi)|\nabla\phi|^2 + \kappa_2\Delta^2\phi$$

(C.8)

□

Curriculum Vitae

Ogochukwu Nneka Ifeacho is the third child and only daughter born to Engr. Francis C. Ifeacho and late Mrs Ogochukwu Ifeacho (Snr.). She attended high school at Holy Rosary International Secondary School Owerri, Imo State, Nigeria, graduated in July 2010.

She got admitted into University of Nigeria, Nsukka in August 2011, graduated in 2015 with a B.Sc in Mathematics. From May 2016-June 2017, she underwent the mandatory National Youth Service Program (NYSC) where she was deployed to Comprehensive Commercial Secondary School as a Mathematics/Physics Teacher.

Due to her passion for Mathematics, she decided to further her studies particularly in the Applied aspect. She began her graduate studies(M.Sc) at The university of Texas at El Paso in August 2018. While pursuing her Master's Program, she worked as a Teaching Assistant and carried out her Thesis research under the supervision of Dr. Natasha Sharma.

She is an active member of the American Mathematical Society (AMS), National Society of Black Engineers(NSBE) and Society of Women Engineers(SWE).

She will be starting her Ph.D in Applied and Industrial Mathematics at New Mexico Institute of Mining and Technology (NMT) in August 2020.

Permanent address: 800 West Yandell Drive

El Paso, Texas 79902.